SUPPORTING INFORMATION

Triazolyl Ru^{II}, Rh^{III},Os^{II} and Ir^{III} Complexes as Potential Anticancer Agents: Synthesis, Structure Elucidation, Cytotoxicity and DNA Model Interaction Studies

Charles K. Rono[1], William K. Chu[1], James Darkwa[1], Debra Meyer[2] and Banothile C.E. Makhubela[1*]

[1]Department of Chemistry, University of Johannesburg, Kingsway Campus, 2006, Auckland Park, SA

[2]Department of Biochemistry, University of Johannesburg, Kingsway Campus, 2006, Auckland Park, SA

Email: bmakhubela@uj.ac.za

NMR Spectra, Single Crystal X-Ray Structures and Mass Spectrometry Data

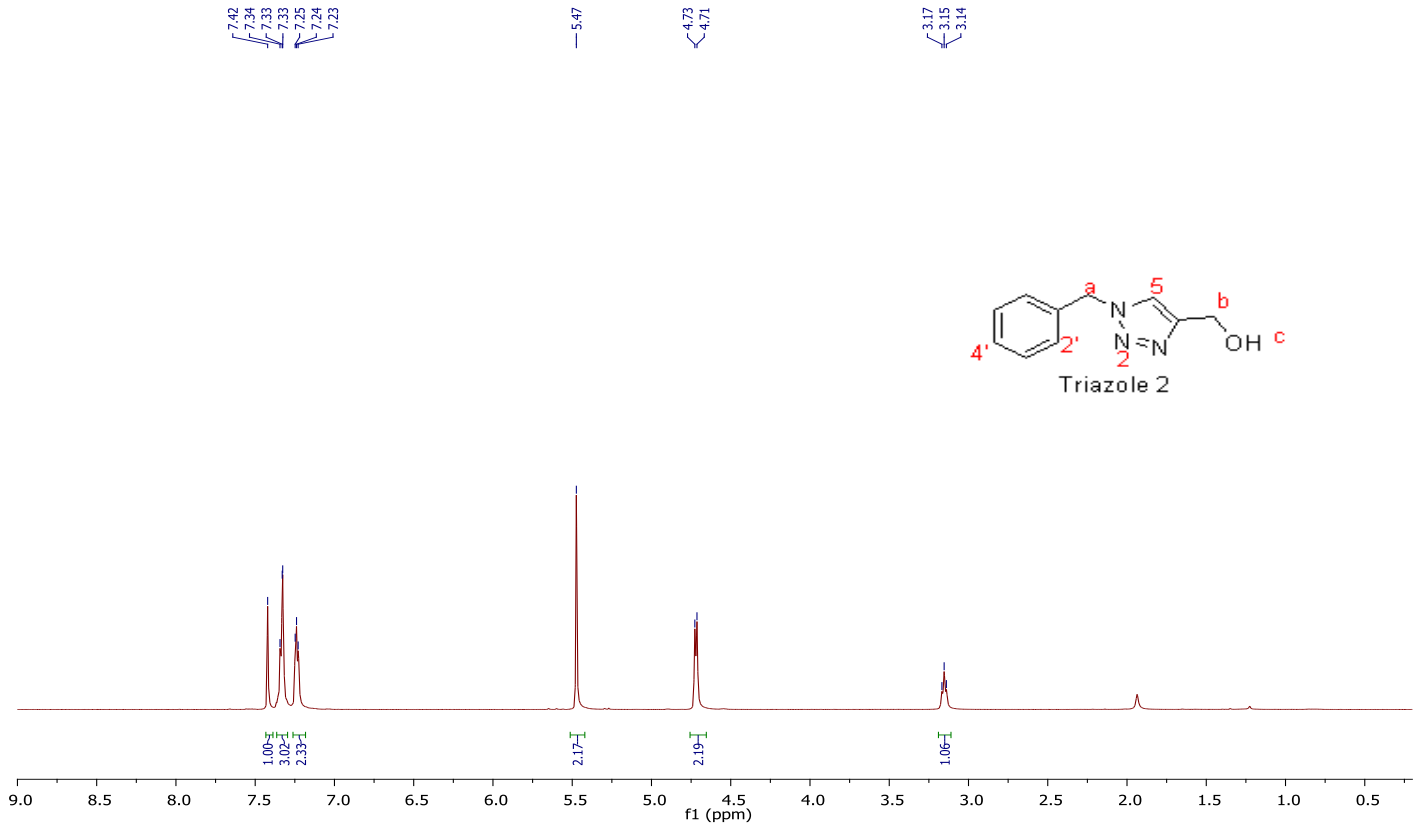

Figure S1: ^{1}H NMR spectrum of the oxidized triazole isomer **2**, 1-benzyl-4-hydroxymethyl-1*H*-1,2,3-triazole in $CDCl_3$ recorded using a 400 MHz FTNMR spectrometer.

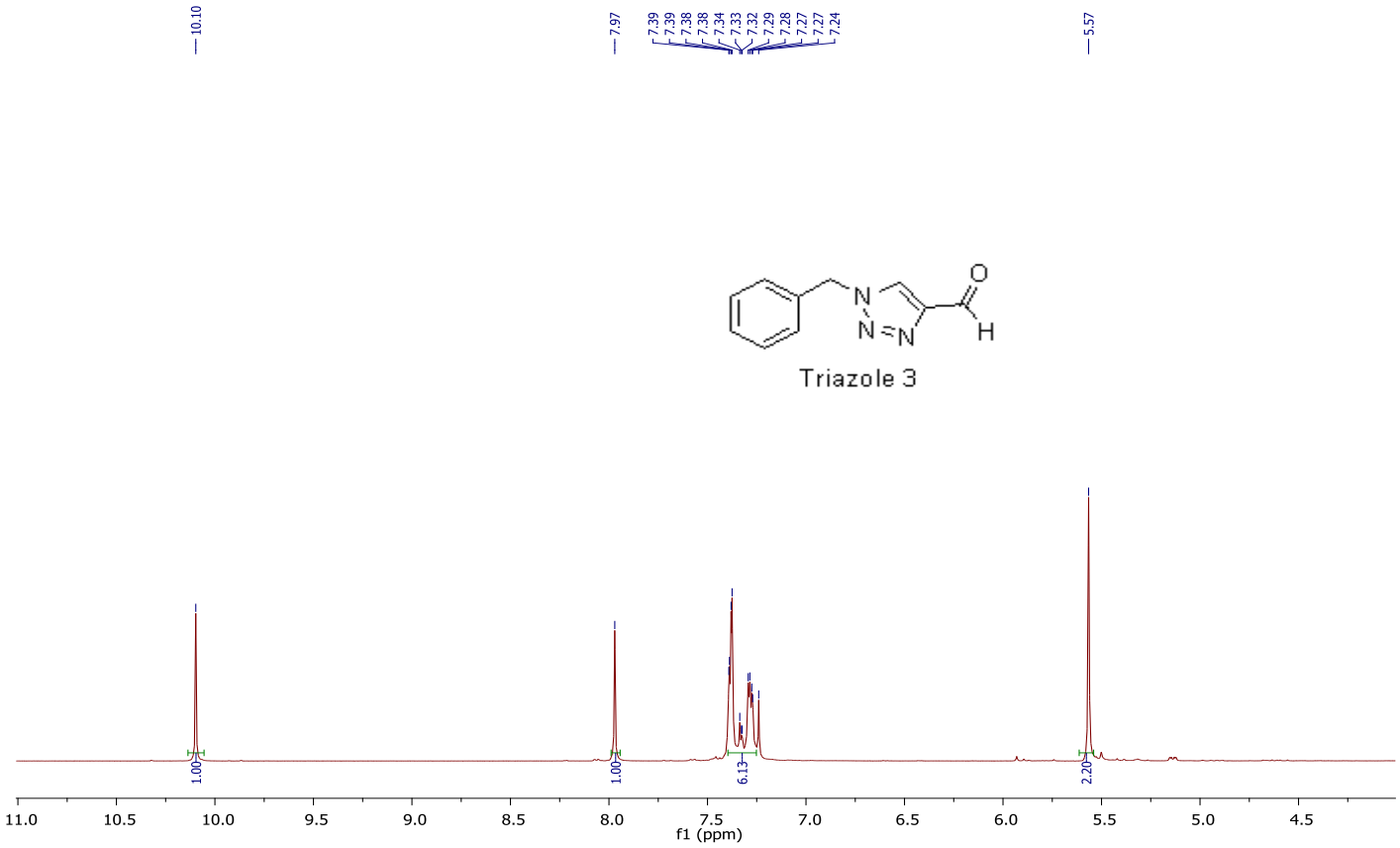

Figure S2: ^{1}H NMR spectrum of the oxidized triazole isomer **3**, 1-benzyl-4-carboxaldehyde-1*H*-1,2,3-triazole, in $CDCl_3$ recorded using a 400 MHz FTNMR spectrometer.

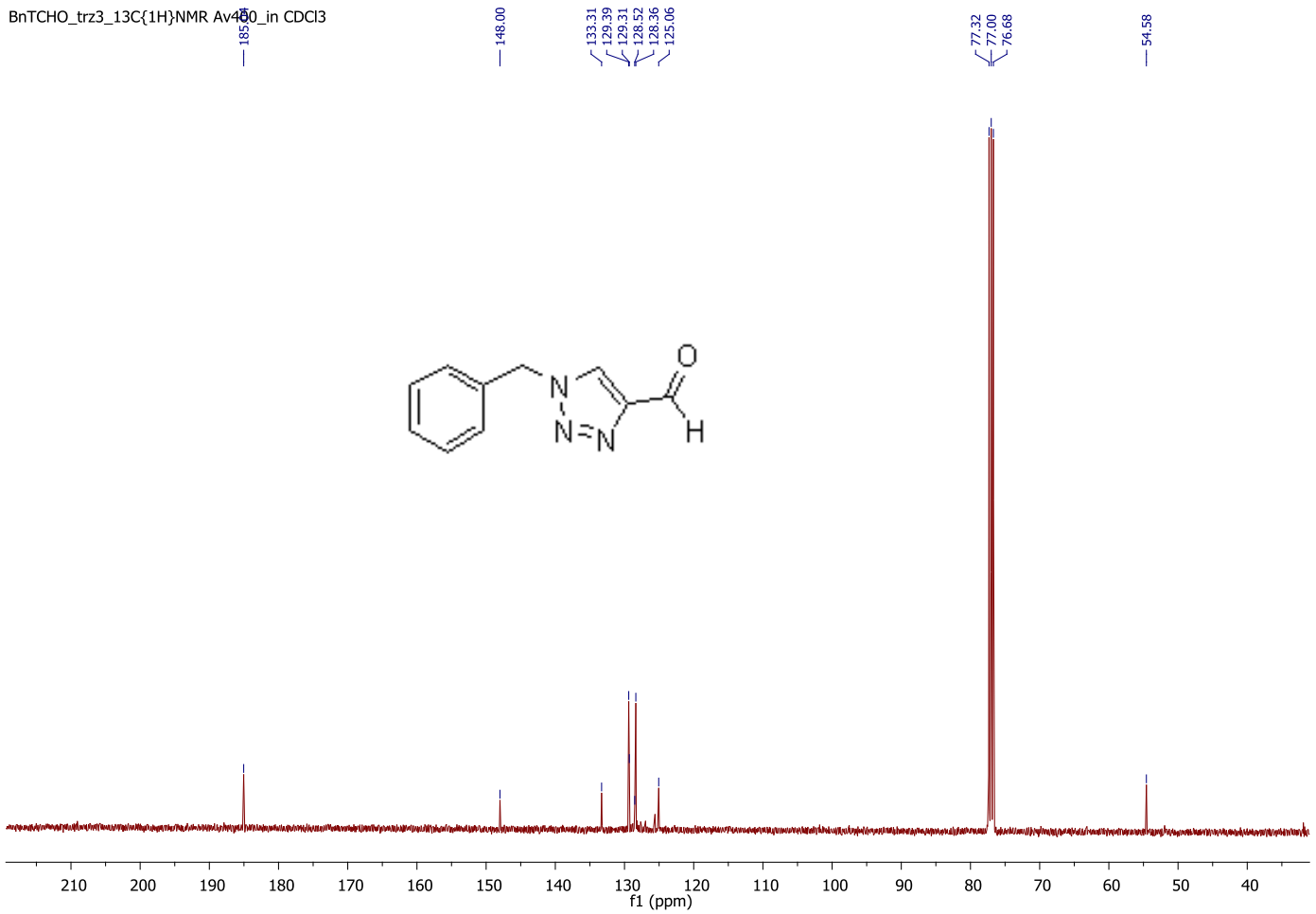

Figure S3: $^{13}C\{^{1}H\}$ NMR spectrum of the oxidized triazole isomer **3**, 1-benzyl-4-carboxaldehyde-1*H*-1,2,3-triazole, in $CDCl_3$ recorded using a 100 MHz FTNMR spectrometer

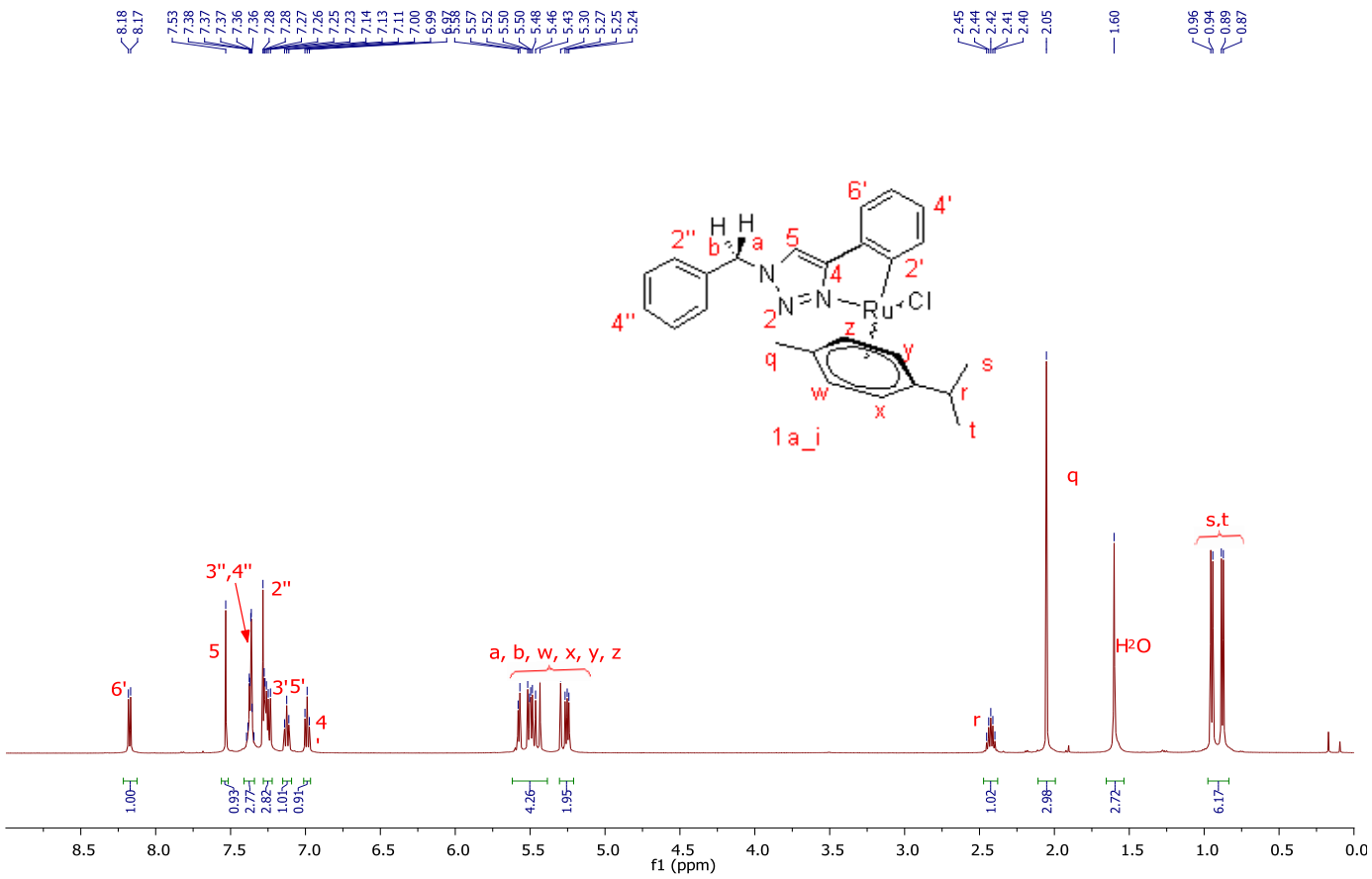

Figure S4: ^{1}H NMR spectrum of stereoisomer **1** of conjugated 1-benzyl-4-phenyl-1*H*-1,2,3-triazolyl(*p*-cymene)ruthenium(II) chloride 5-membered metallacycle, **1a_I**, in $CDCl_3$ recorded using a 500 MHz FTNMR spectrometer.

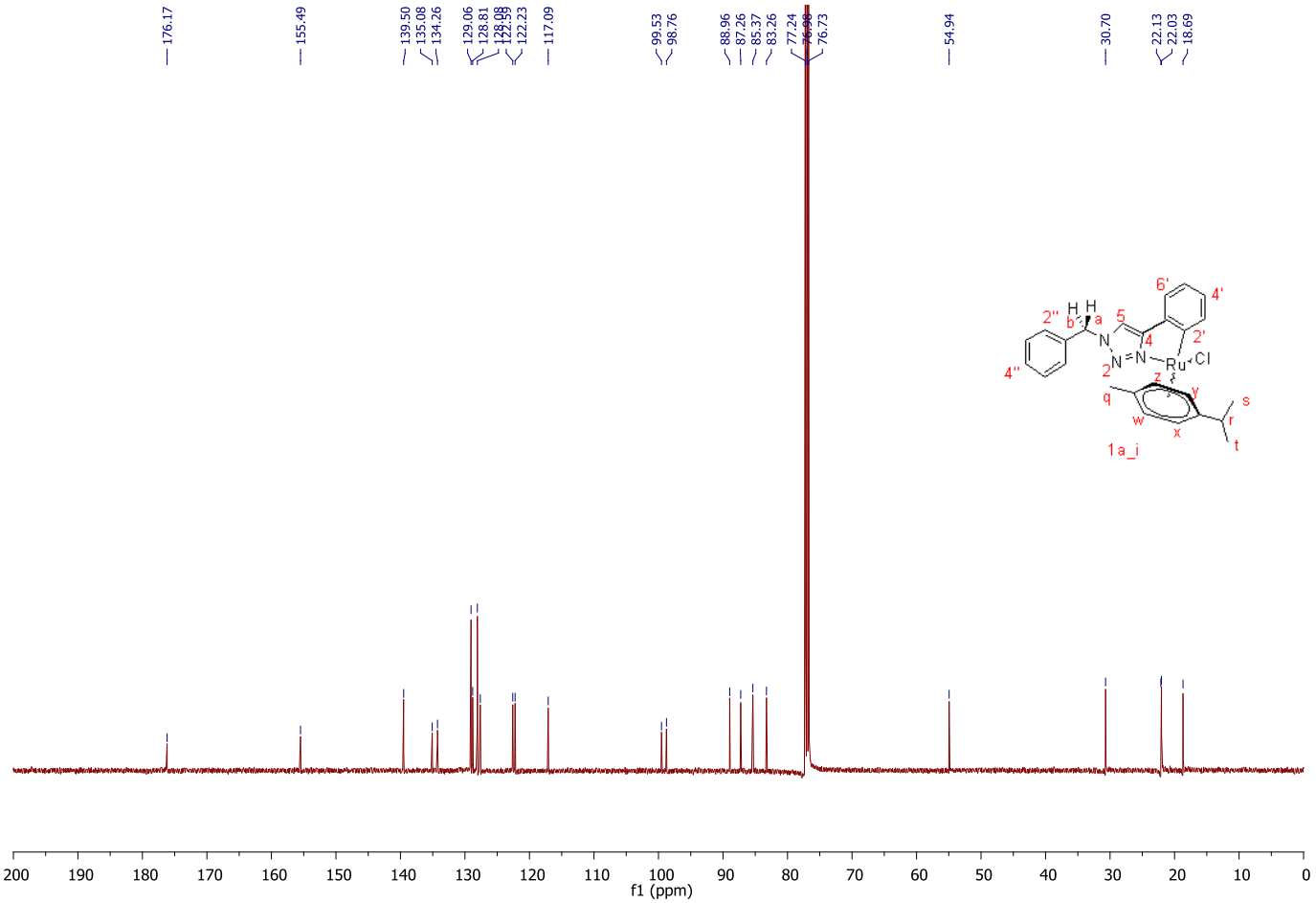

Figure S5: $^{13}C\{^{1}H\}$ NMR spectrum of stereoisomer **I** of conjugated1-benzyl-4-phenyl-1*H*-1,2,3-triazolyl(*p*-cymene)ruthenium(II) chloride 5-membered metallacycle, **1a_I**, in $CDCl_3$ recorded using a 125 MHz FTNMR spectrometer.

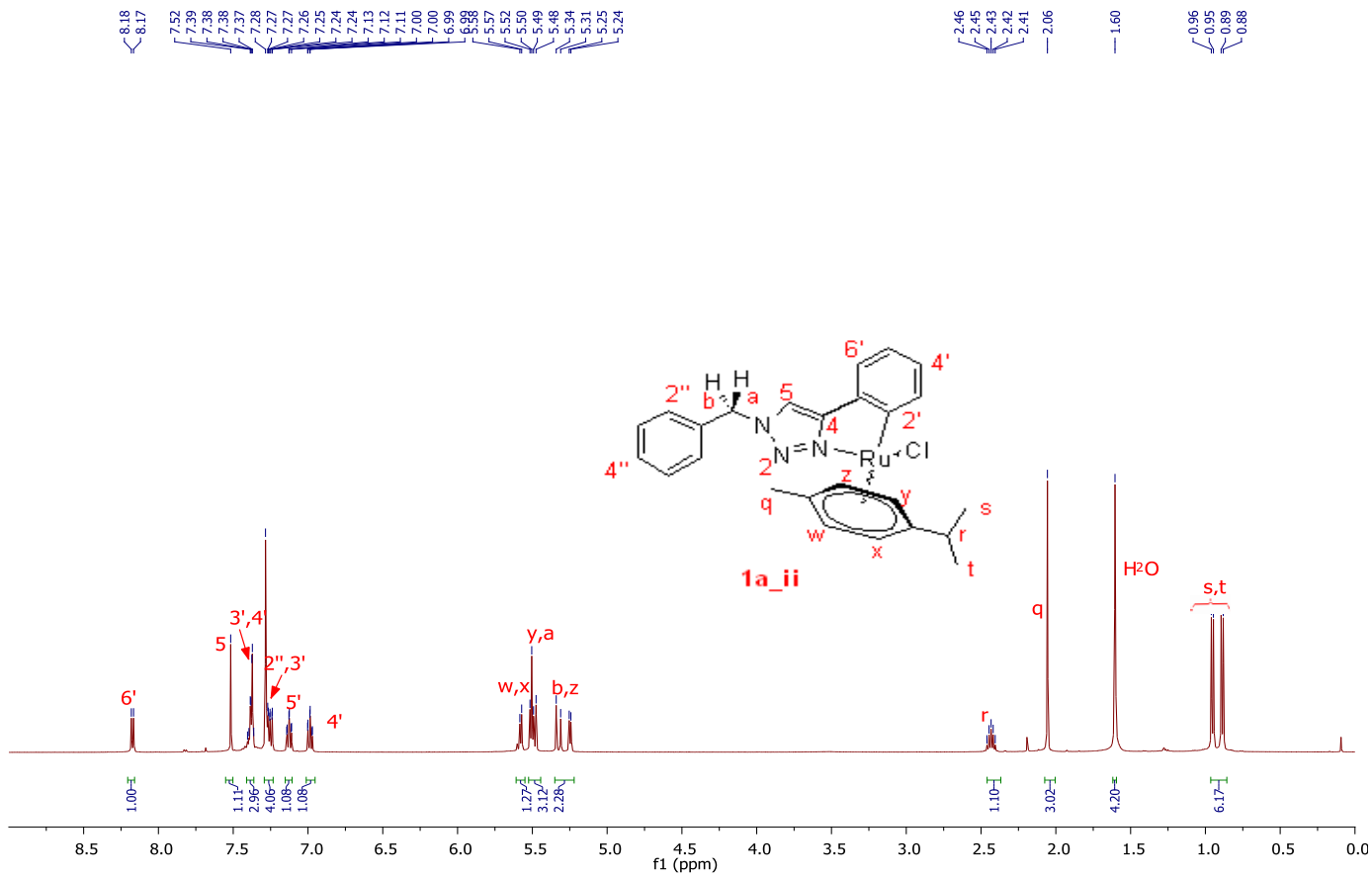

Figure S6: ^{1}H NMR spectrum of stereoisomer **II** of conjugated 1-benzyl-4-phenyl-1*H*-1,2,3-triazolyl(*p*-cymene)ruthenium(II) chloride 5-membered metallacycle, **1a_II**, in $CDCl_3$ recorded using a 500 MHz FTNMR spectrometer.

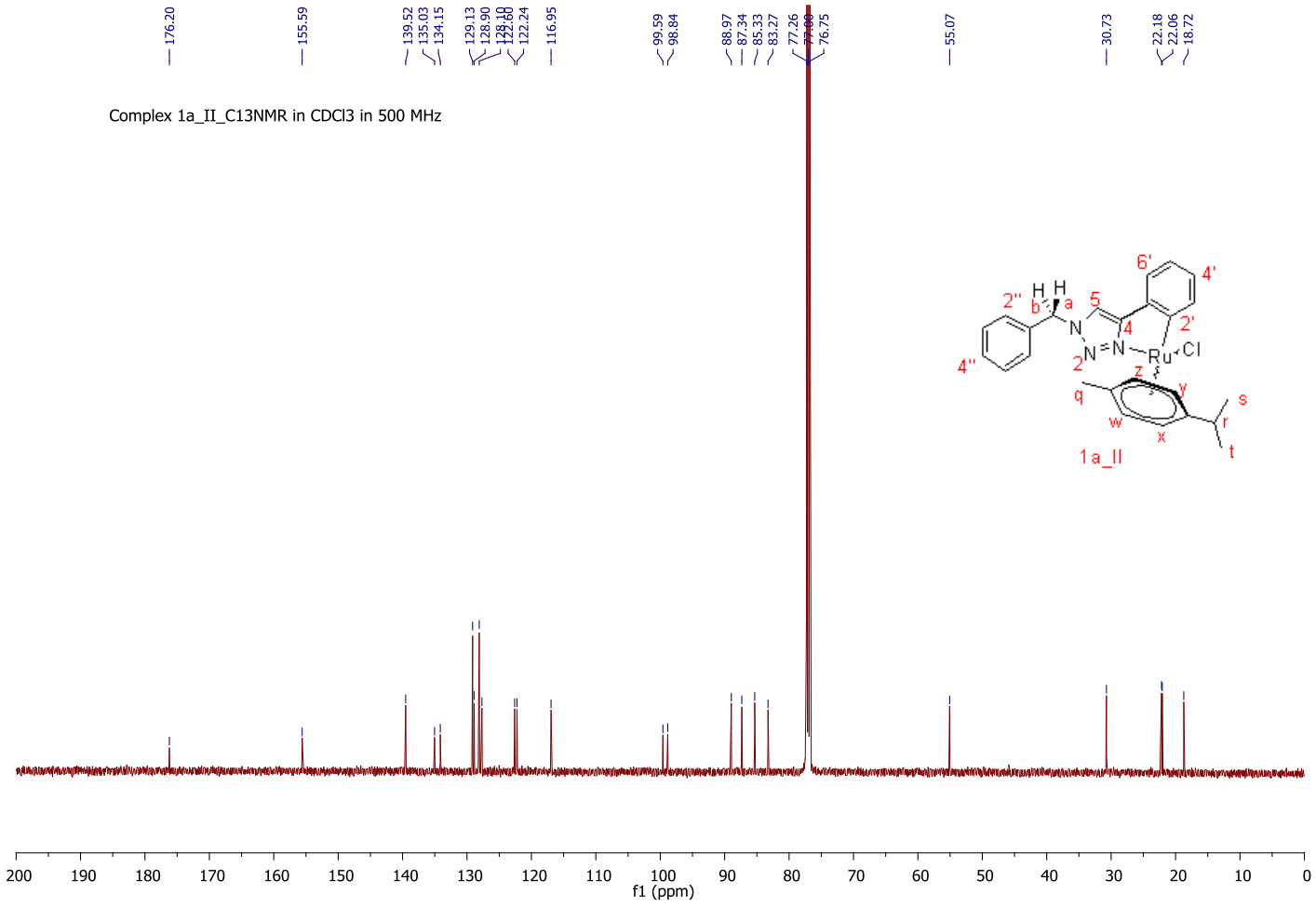

Figure S7: $^{13}C\{^{1}H\}$ NMR spectrum of stereoisomer **II** of conjugated 1-benzyl-4-phenyl-1*H*-1,2,3-triazolyl(*p*-cymene)ruthenium(II) chloride 5-membered metallacycle, **1a_II**, in $CDCl_3$ recorded using a 125 MHz FTNMR spectrometer.

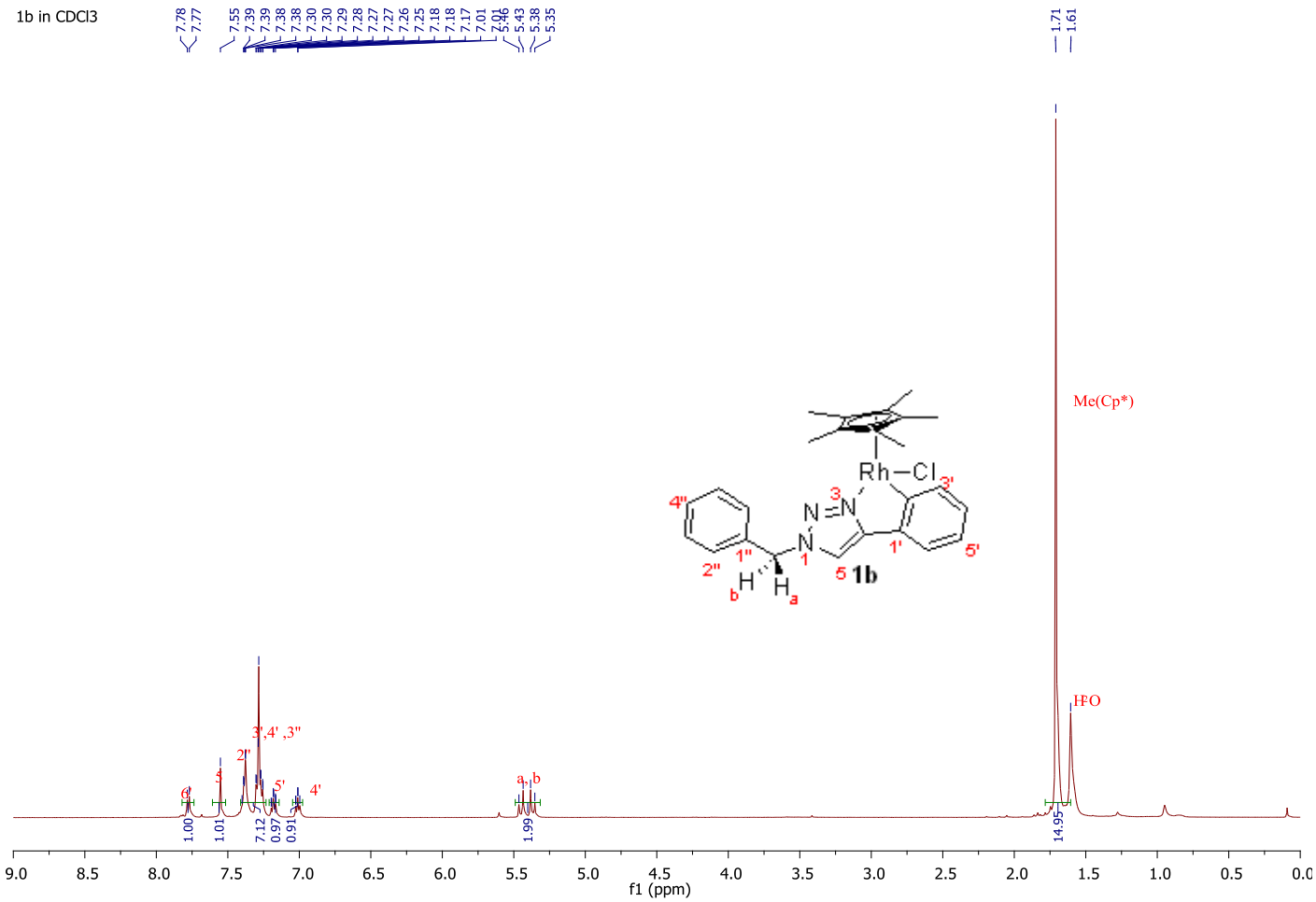

Figure S8: ^{1}H NMR spectrum of 1-benzyl-4-phenyl-1*H*-1,2,3-triazolyl-(pentamethylcyclopentadienyl)rhodium(III) chloride complex **1b** in $CDCl_3$ recorded using a 400 MHz FTNMR spectrometer.

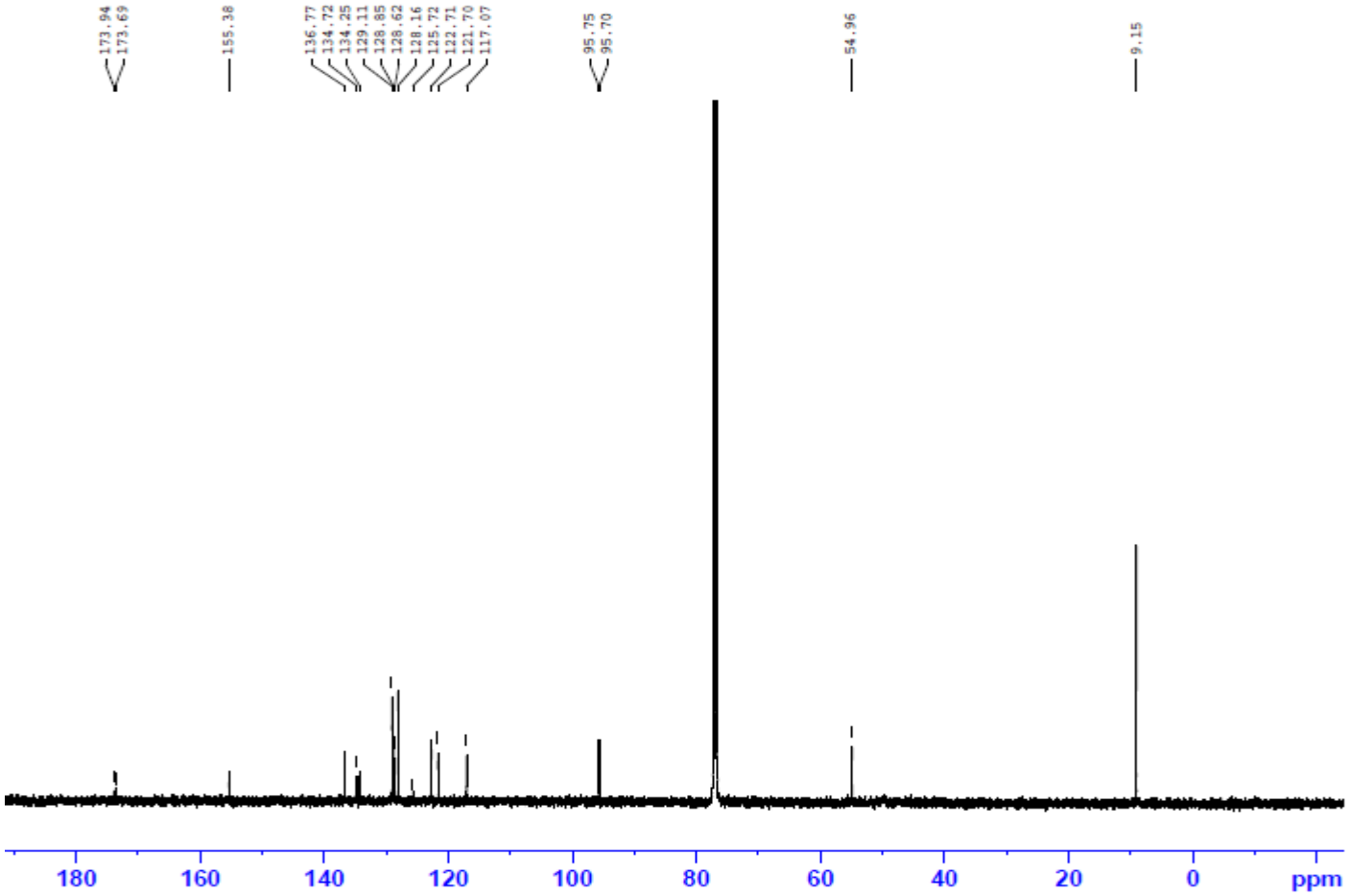

Figure S9: $^{13}C\{^{1}H\}$ NMR spectrum of 1-benzyl-4-phenyl-1*H*-1,2,3-triazolyl-(pentamethylcyclopentadienyl)rhodium(III) chloride, complex **1b** in $CDCl_3$ recorded using a 100 MHz FTNMR spectrometer.

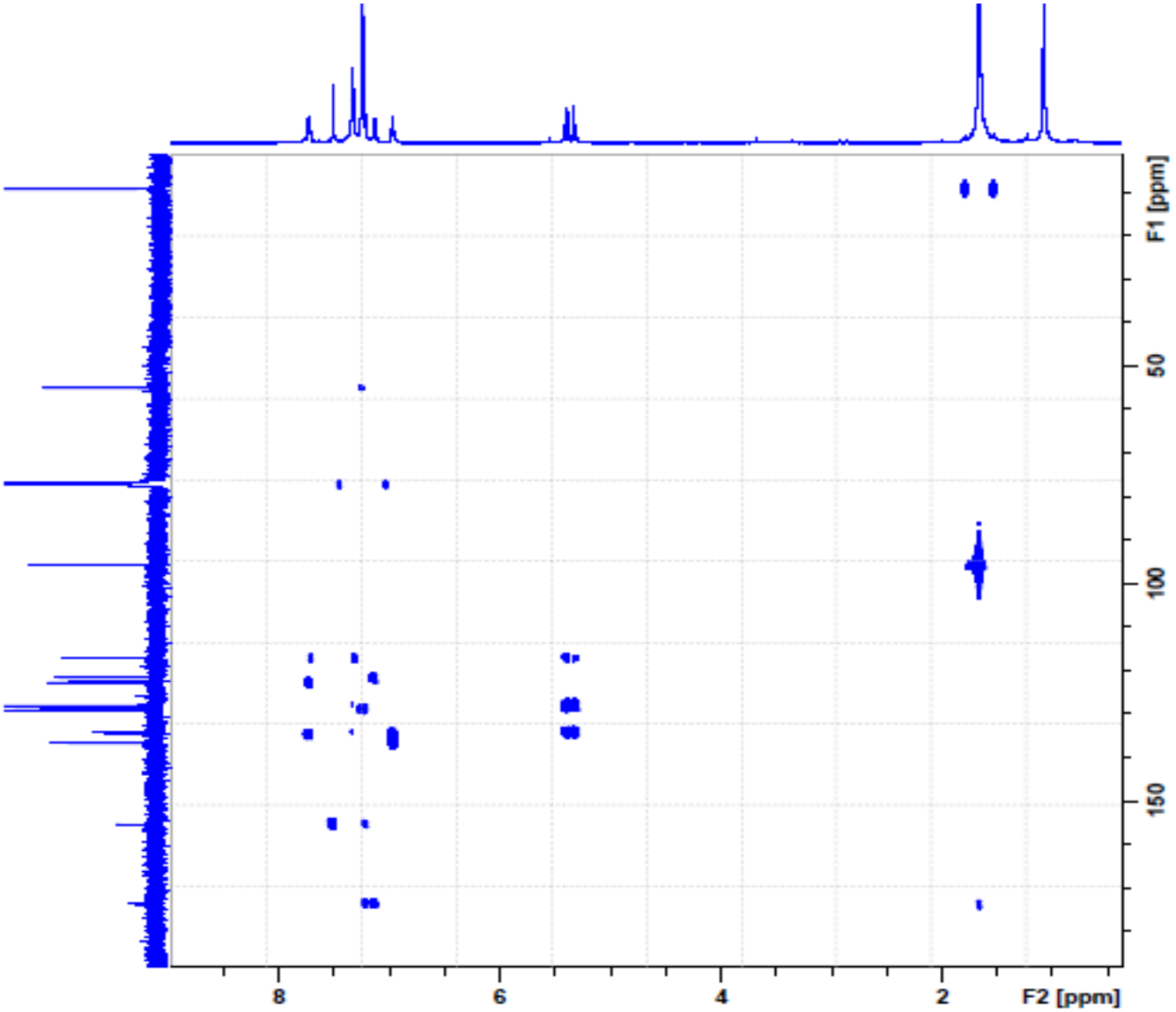

Figure S10: ^{1}H-^{13}C HMBC spectrum showing cross-peaks of protons (H) in through (two-to-four) bonds correlations with neighboring carbon atoms correlations in rhodium(III) cyclometalate **1b** in $CDCl_3$ recorded using a 500 MHz FTNMR spectrometer.

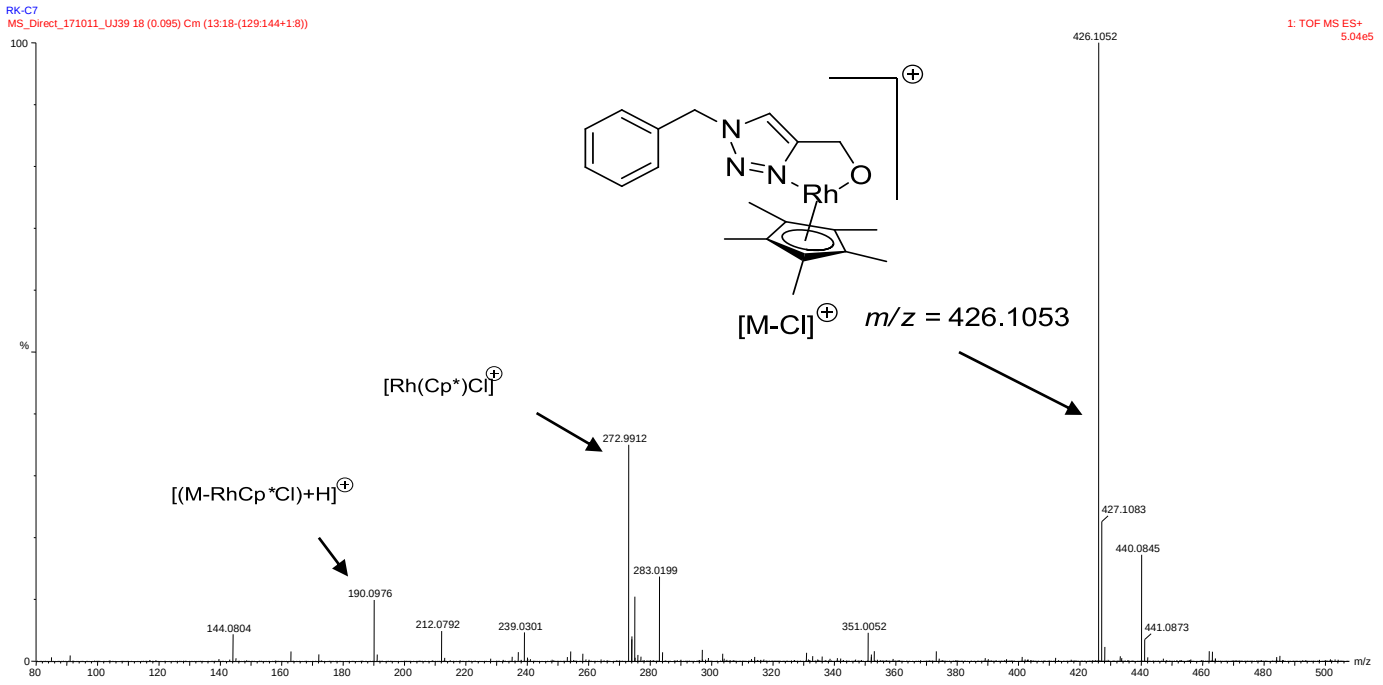

Figure S11: HRMS-ESI spectrum of conjugated 1-benzyl-4-methyloxy-1*H*-1,2,3-triazolyl(1,2,3,4,5-pentamethylcyclopentadienyl)rhodium(III) chloride complex, **2b**.

Table S1: Selected NOESY ^{1}H-^{1}H correlations in complex 1b and 1b-5'-GMP and ^{1}H-^{13}C HMBC for 1b

Chemical Shift, δ (ppm)			
H	**NOESY (^{1}H-^{1}H)**		**HMBC (^{1}H-^{13}C)**
	1b	**1b-5'-GMP**	**1b**
5.3	7.32, 7.52	7.32, 4.3(GMP)	117.0 (C-5), 128.6 (C-2"), 134.2 (C-1")
6.96	7.13	7.13	134.7 (C-1'), 136.7 (C-6')
7.13	6.96	6.96	121.7 (C-3'), 173.7 (C-2'(Rh))
7.32	5.3	H8 (Im), 5.3	128.1 (C-3"), 134.2(C-1")
7.51	5.3		117.0 (C-H, dd, 1JCH = Hz), 54.9
7.73	1.66 Me (Cp*)	1.66 Me(Cp*)	122.7 (C-3'), 134.7 (C-1')

SUPPORTING INFORMATION

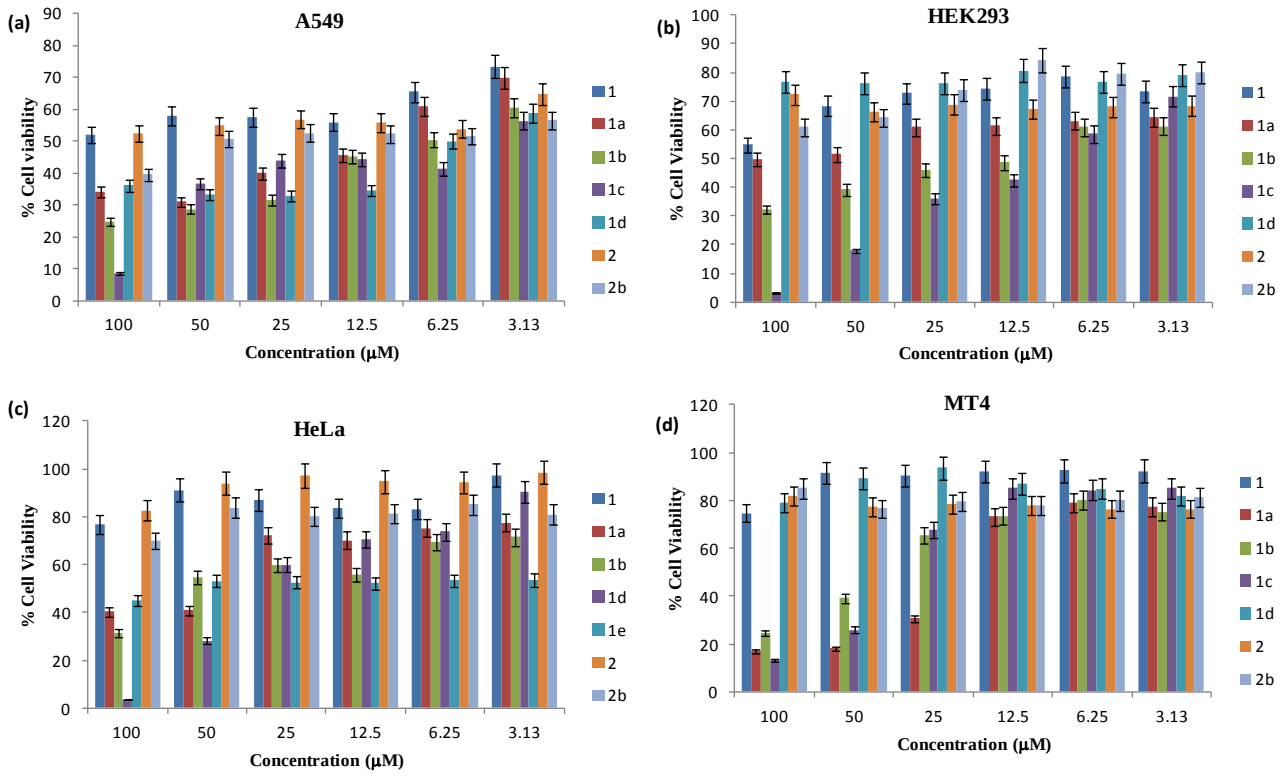

Figure S12: Colorimetric MTS assay results for the triazolyl conjugated complexes (**1**(**a-d**) and **2b**) evaluated against MT4 (leukemia), HeLa (cervical), HEK293 (kidney adenocarcinoma) and A549 (lung cancer) cell lines at six two-fold dilutions (100 µM, 50 µM, 25 µM, 12.5 µM, 6.25 µM and 3.13 µM). The data was collected in duplicate for three independent measurements and reported as mean ± SEM with n = 6, with the plus caps representing the standard error of mean bars. Auranofin was used as the positive control.

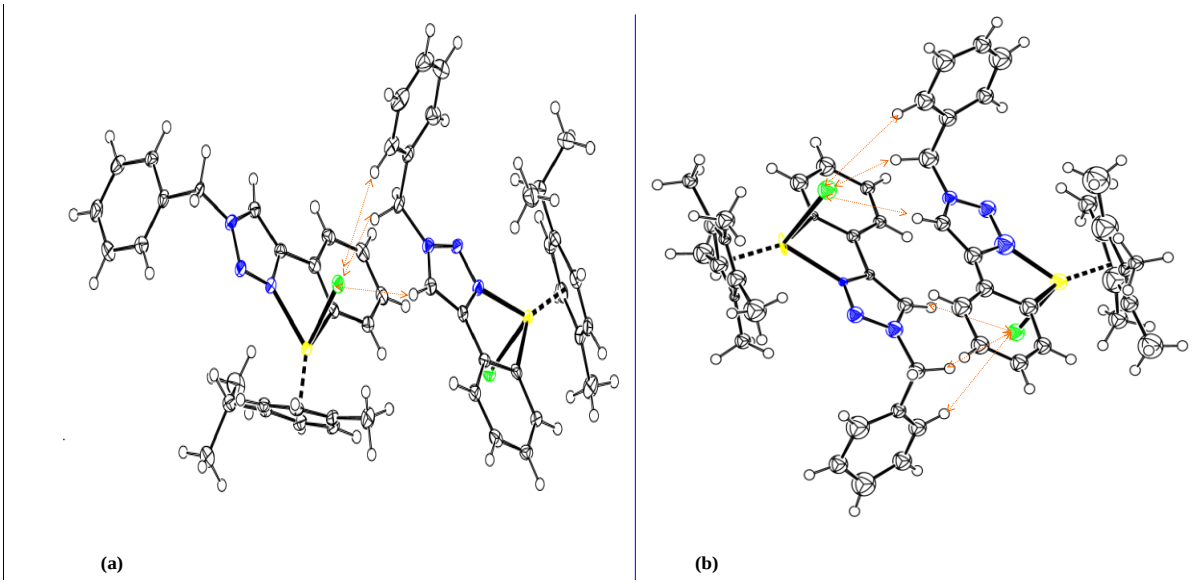

Figure S13: Displacement thermal ellipsoids plot with 50 % probability of the dimeric units in the molecular structures of 1-benzyl-4-phenyl-1*H*-1,2,3-triazolyl **(a)** (*p*-cymene)ruthenium(II) dichloride complex, **1a** and **(b)** (pentamethylcyclopentadienyl)iridium(III) chloride, **1c**.

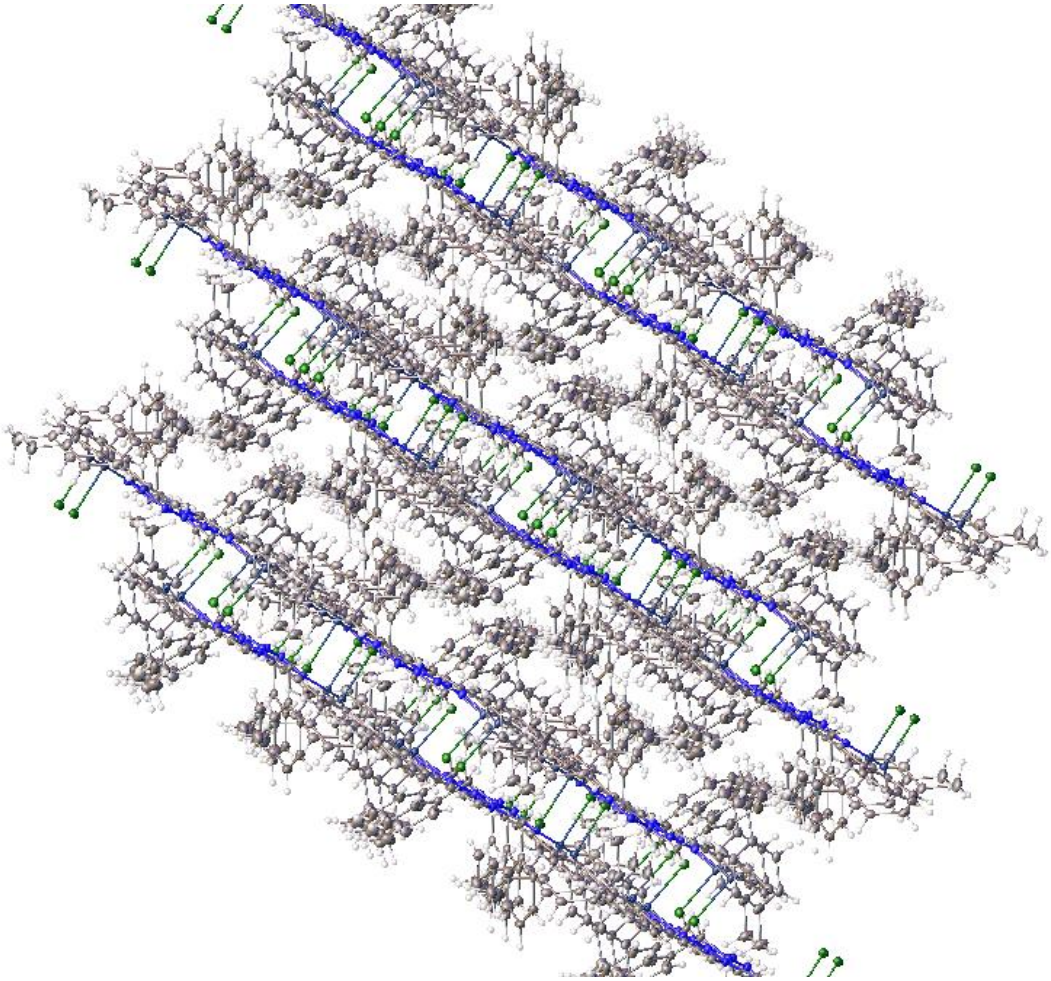

Figure S14: Molecular packing in the crystal structure of 1-benzyl-4-phenyl-1*H*-1,2,3-triazolyl (*p*-cymene)ruthenium(II) dichloride complex, **1a**.

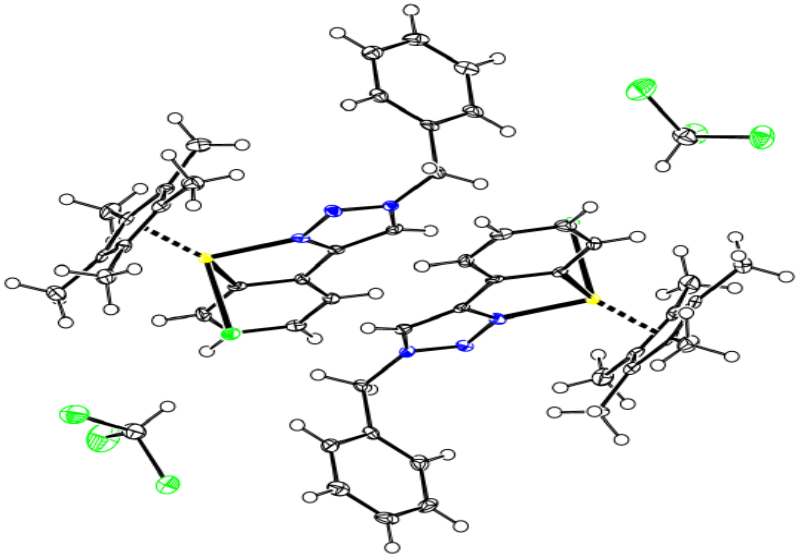

Figure S15: Displacement thermal ellipsoids plot with 50 % probability of the dimeric units in the molecular structures of 1-benzyl-4-phenyl-1*H*-1,2,3-triazolyl (pentamethylcyclopentadienyl)rhodium(III) chloride, **1b,** which co-crystallized with chloroform.

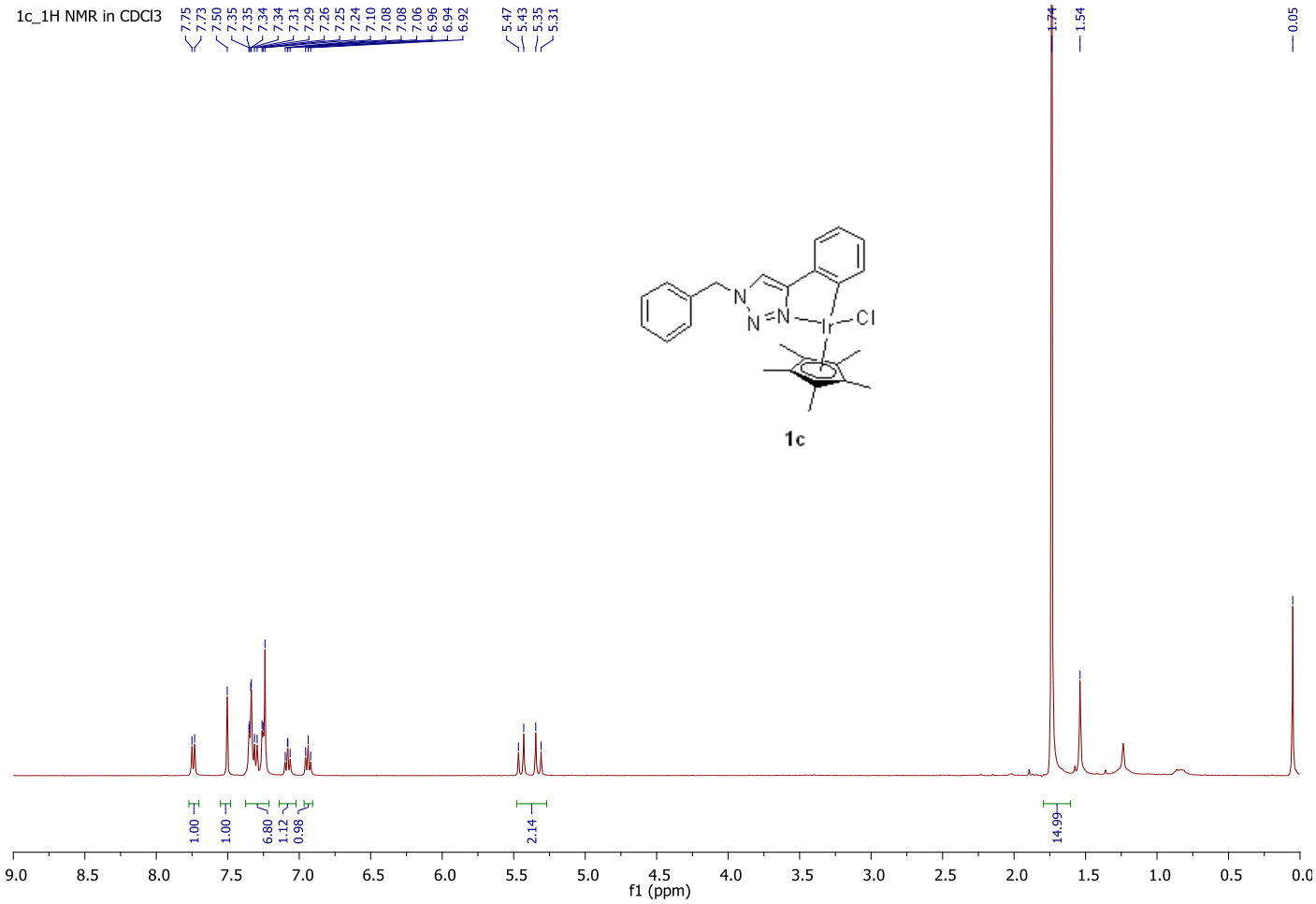

1c

Figure S16: ^{1}H NMR spectrum of 1-benzyl-4-phenyl-1*H*-1,2,3-triazolyl-(pentamethylcyclopentadienyl)iridium(III) chloride complex **1c** in $CDCl_3$ recorded using a 400 MHz FTNMR spectrometer.

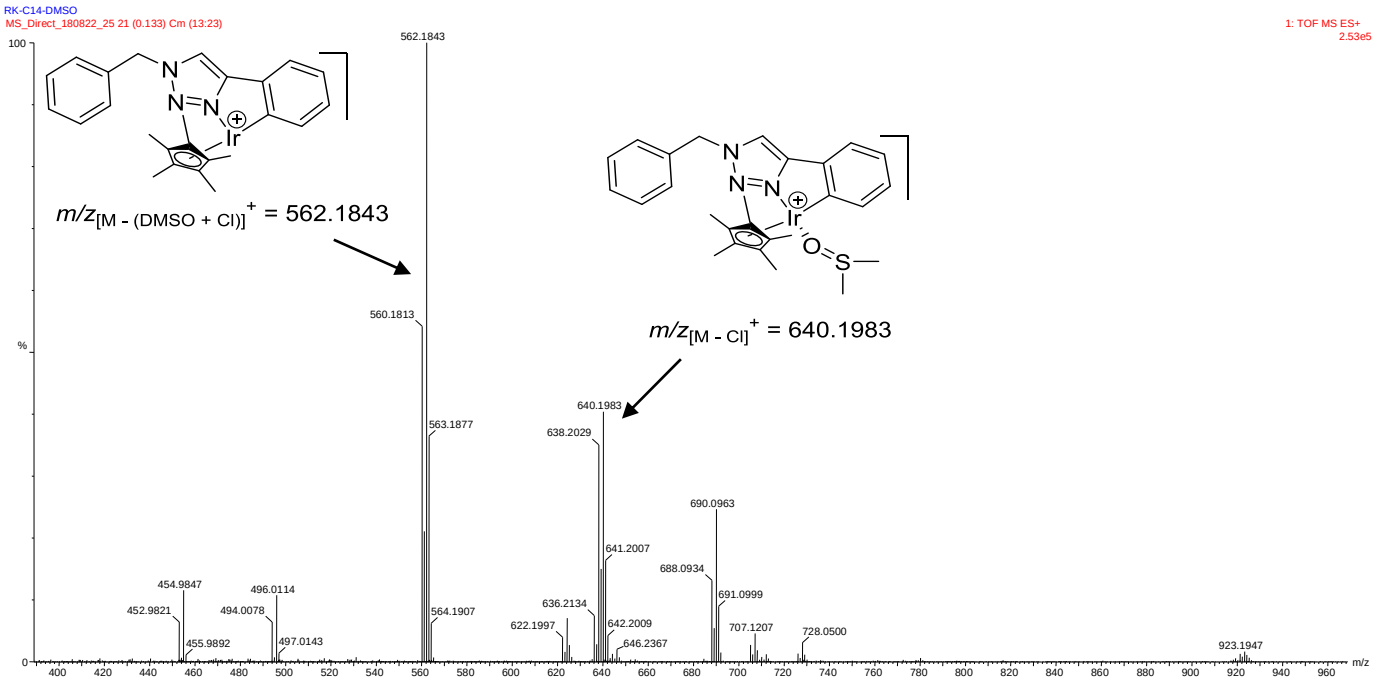

Figure S17: HRMS-ESI spectrum for cyclometallated 1-benzyl-4-phenyl-1*H*-1,2,3-triazolyl (pentamethylcyclopentadienyl)(DMSO)iridium(III) chloride cationic complex, **1c-dmso**, obtained by incubation of iridacycle **1c** in dimethyl sulfoxide and water solvent system at 313 K.

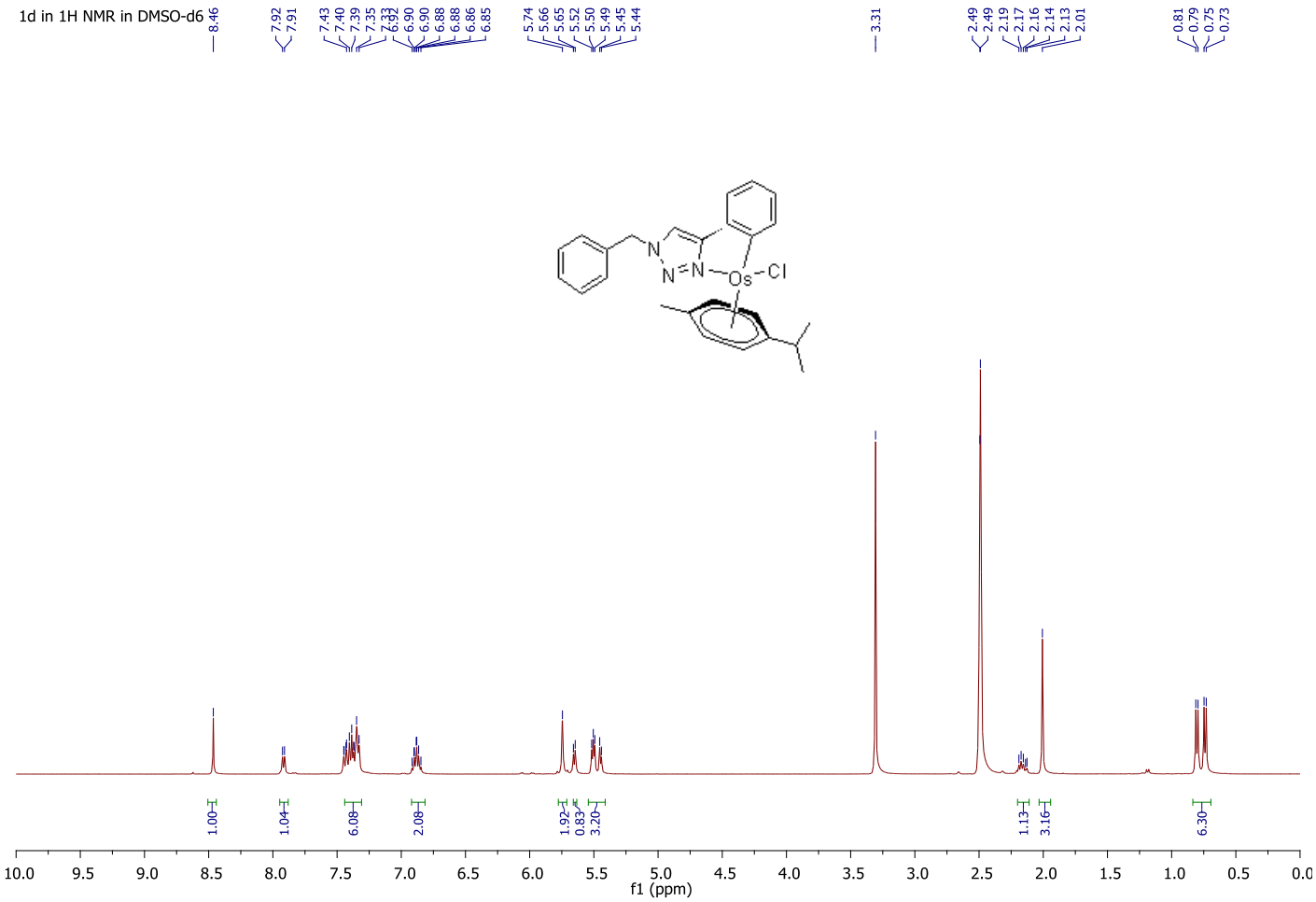

Figure S18: ^{1}H NMR spectrum of conjugated 1-benzyl-4-phenyl-1*H*-1,2,3-triazolyl (*p*-cymene)osmium(II) chloride 5-membered metallacycle, **1d**, in DMSO-d_6 recorded using a 400 MHz FTNMR spectrometer.

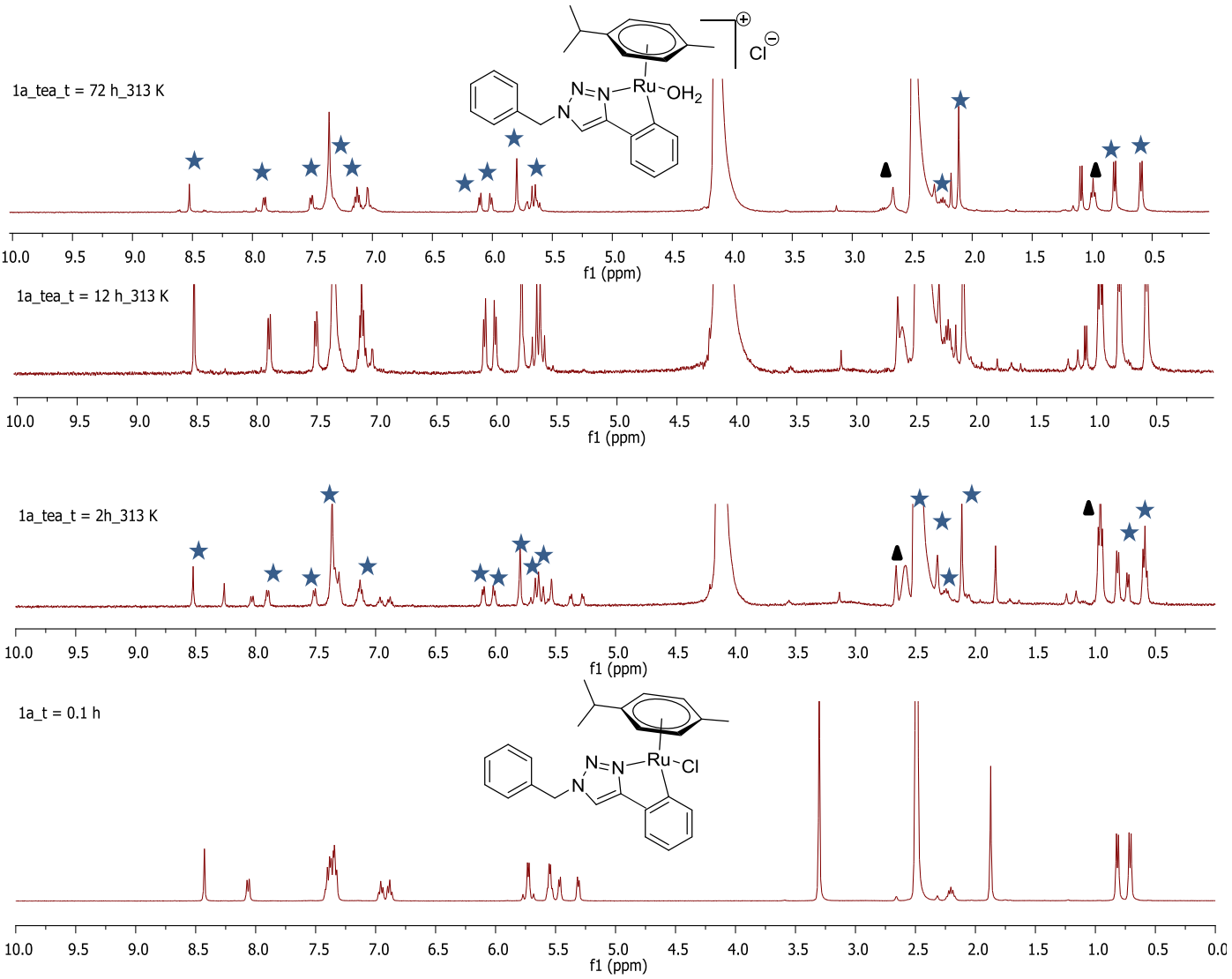

Figure S19: Time dependent ^{1}H NMR spectra showing the formation of aquated complex of **1a** in the presence of triethyl amine (▲) recorded in DMSO-d_6 in D_2O using a 400 MHz FTNMR spectrometer. At t = 0.1 h, the neutral chloride complex **1a** (lower spectrum) is the predominant species; after 2 h of incubation of complex 1a in aqueous conditions, the cationic aquated complex 1a (★) is almost in equilibrium with the neutral complex **1a** while the cationic aquated complex 1a is the predominant species after t = 12 h. There was no detectable deprotonation of the triazolyl proton H-5 in both the neutral complex **1a** and the cationic aquated complex of **1a**.

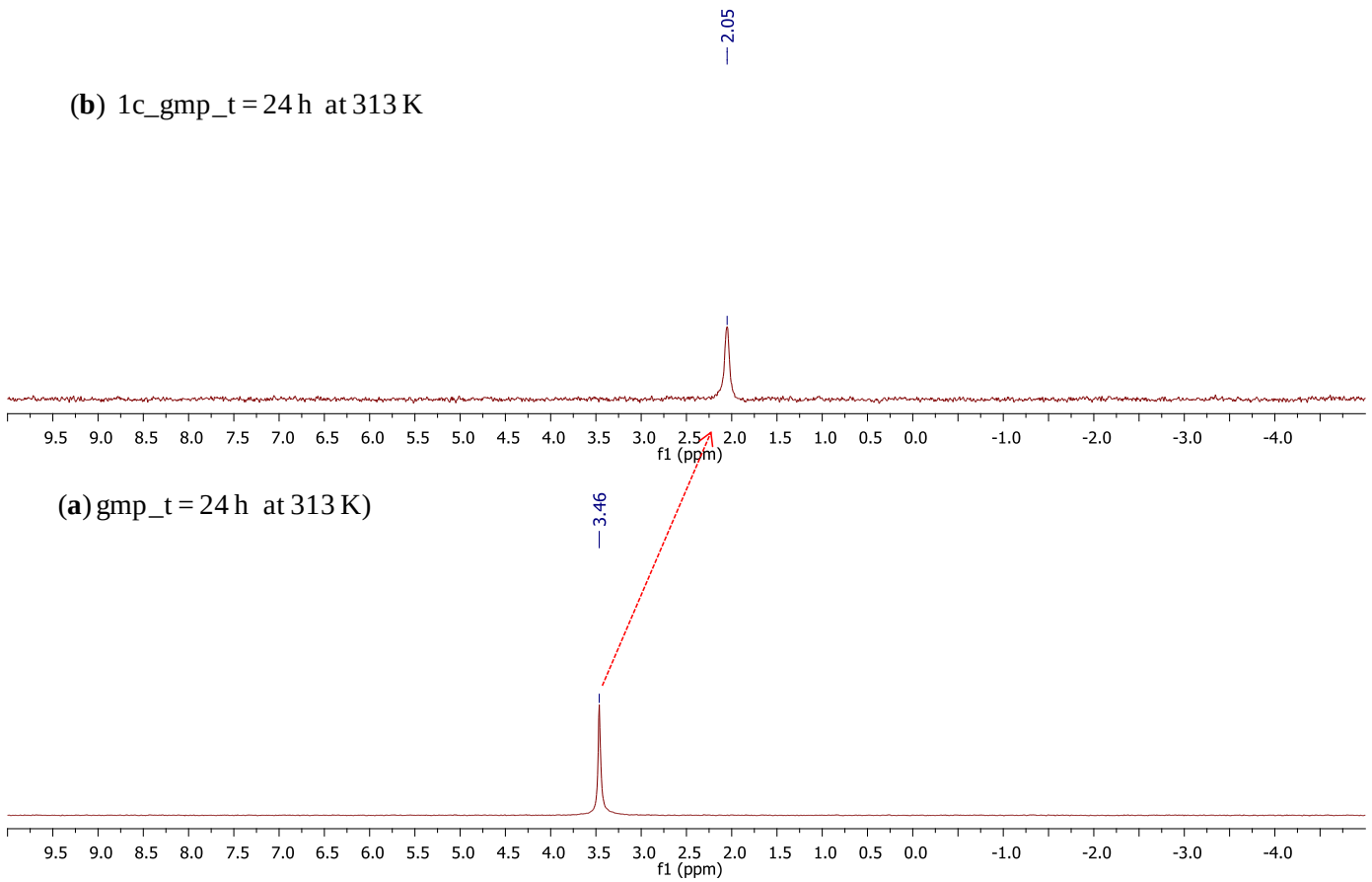

Figure S20: $^{31}P\{^{1}H\}$ NMR (202 MHz, DMSO-d_6) showing an upfield shift ($\Delta\delta$ = -1.41 ppm) in the phosphorous peak of DNA model guanosine 5'-GMP upon incubation with complex **1c** at 313 K for 24 h in the process of carbenylation. (a) $^{31}P\{^{1}H\}$ NMR (202 MHz, DMSO-d_6) of free DNA model guanosine 5'-GMP (b) $^{31}P\{^{1}H\}$ NMR (202 MHz, DMSO-d_6) of **1c**-5'-GMP complex upon after 24 h of incubation at 313 K.

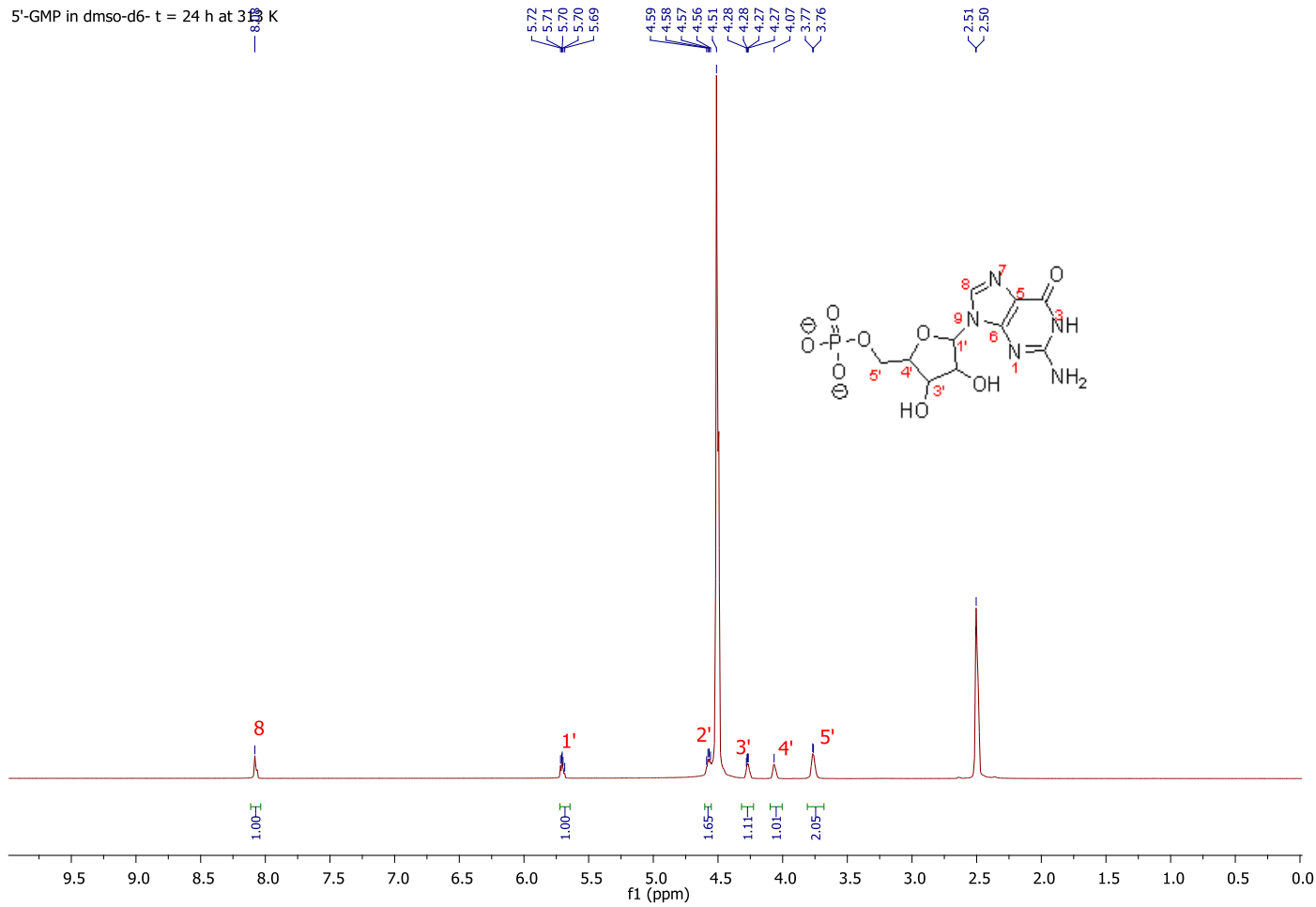

Figure S21: ^{1}H NMR (500 MHz, DMSO-d_6) of DNA model guanosine 5'-GMP upon incubation with complex **1c** at 313 K for 24 h.

SUPPORTING INFORMATION

Incubation of complex 1c with 2-methylimidazole

In a typical experiment, an aqueous solution (0.2 mL) of 2-methylimidazole (0.45 mg, 1.0 equiv) was added in one portion to an incubating aqueous solution of aquated complex **1c** (3 mg, 5.0 x 10^{-3} mmol, 1.0 equiv) in 50 % DMSO-d_6 in mQH_2O at 313 K. Subsequently, the ^{1}H NMR spectrum of the complex solution was recorded immediately, then at intervals of 12 h for a period of 120 h. **Figure S22** (ESI) shows selected ^{1}H NMR spectra of the complex mixture after 2 h, 24 h and 48 h as supportive evidence of the formation of k^1N-1c-2MeIm complex isomeric mixture (*). There was no significant difference between the spectra recorded after 2 h and that of 12 h as well as between 48 h and 120 h of incubation.

Scheme S1: Incubation of complex **1c** and 2-methylimidazole mixture forms k^1N-1c-2MeIm complex

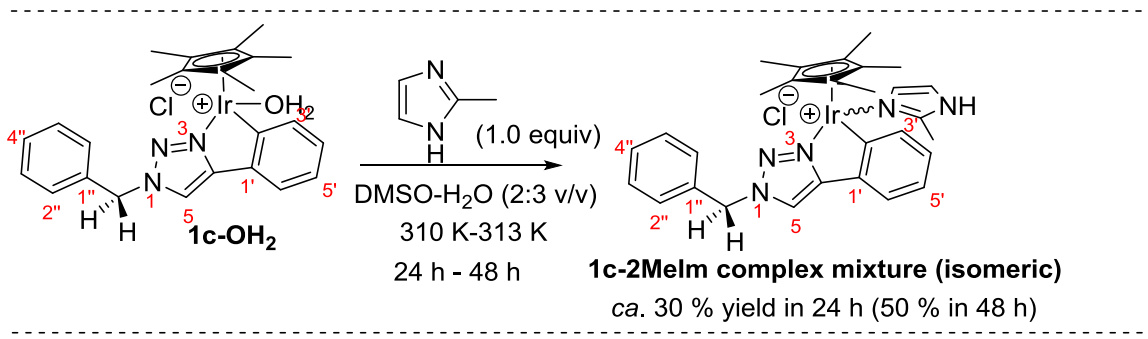

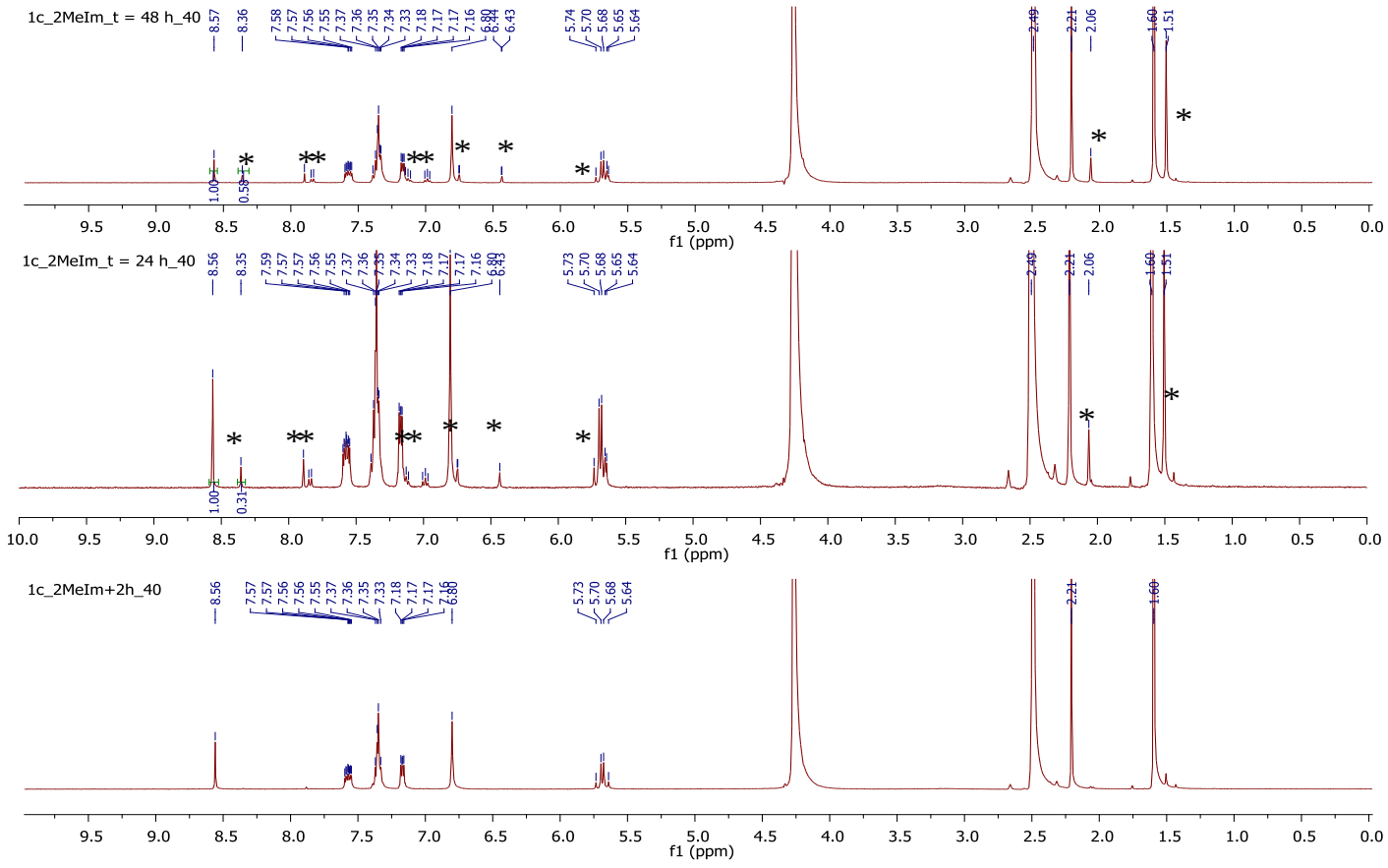

Figure S22: ^{1}H NMR spectra (400MHz, DMSO-d_6) upon incubation of complex **1c** with 2-methylimidazole for 48 h at 313 K; showing the emergence and growth of k^1N-1c-2MeIm coordination complex of **1c** (*) recorded after 2 h, 24 h and 48 h of incubation.

SUPPORTING INFORMATION

p*Ka* determination. A plot of pH versus the resonance shift of the methylene protons was obtained by incubation of the mixture for about 12 h at 313 K (**Figure S23**).

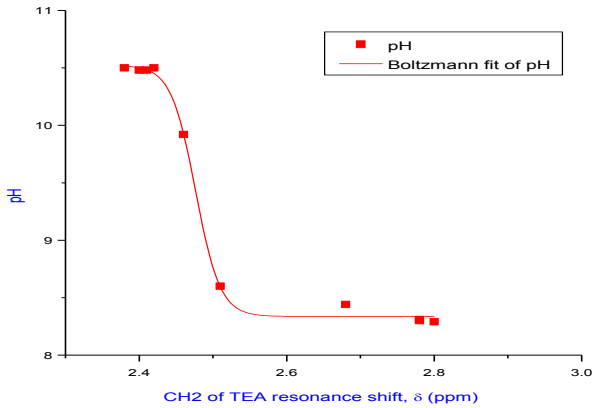

Figure S23: Scatter plot of pH *versus* resonance shift, δ, of te C$\underline{H_2}$ in triethyl amine obtained over duration of 12 h following deprotonation of triazole proton H-5 in complex **1c** upon incubation at 313 K for 12 h with pH curve fitted using Boltzmann fitting model (R^2 = 0.9974; p*K*a of triazole H-5 of **1c** is *ca.* 9.4 from the inflection point of the curve).

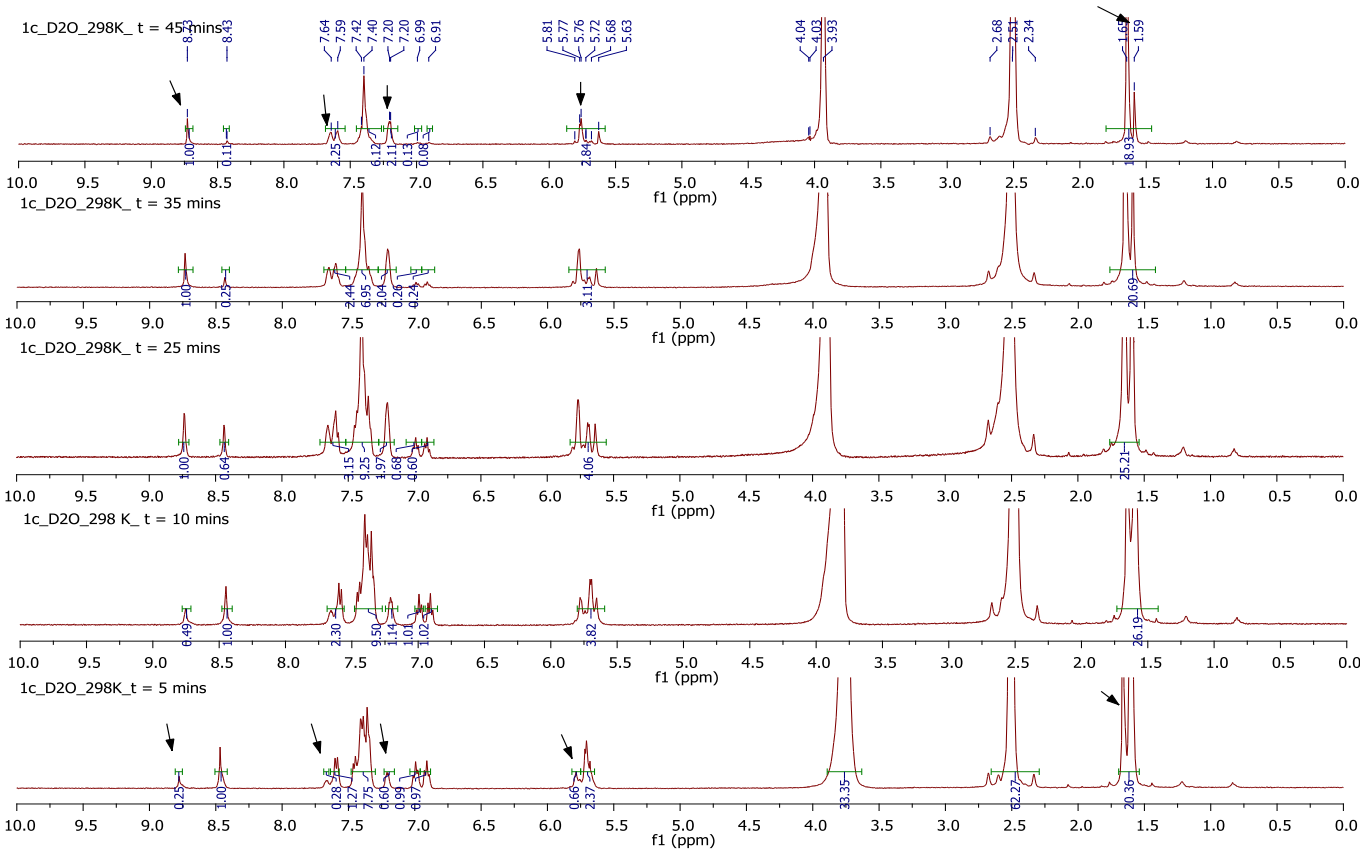

Figure S24: Time dependent ^{1}H NMR of complex **1c** showing the conversion of the chloride complex **1c** (major compound at t = 5 mins; δ_H = 8.43 ppm) to the aquated complex **1c** (major compound at t = 45 mins; δ_H = 8.43 ppm, shown by arrows). The spectrum was recorded in dmso-d_6 using 400 MHz FTNMR. The spectrum recorded at t = 5 mins shows the emergence of a new set of signals corresponding to aquated complex **1c** (shown by arrows) each downfield with respective to that chloride complex **1c**.

SUPPORTING INFORMATION

Behavior of complex 1a and 1c in aqueous environment in the presence of amino acids: Interaction of these complexes with amino acids, L-cysteine, L-Proline, DL-proline and L-histidine were evaluated for an extended duration of 168 h – 240 h at incubation temperature of 313 K. **Figure S25** shows an overlay of the ^{1}H NMR spectra of the aquated complex **1c**, **1c**+proline and 1c+cysteine. **Figure S26** and **S27** show ^{1}H NMR spectra of complex **1c** and **1a** respectively with histidine as one of the representative amino acids containing potentially coordinating imidazole moiety.

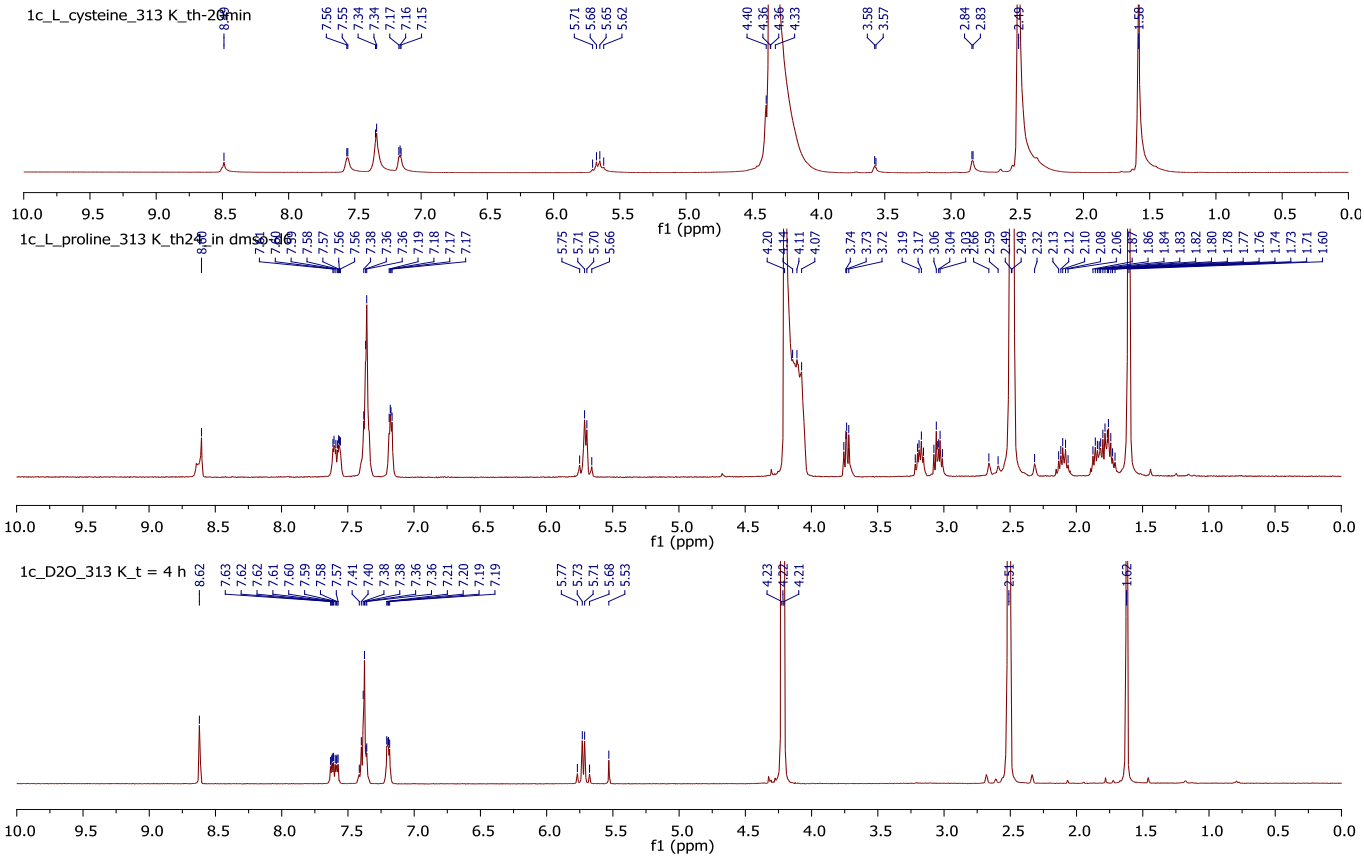

Figure S25: Comparison of time dependent ^{1}H NMR (500MHz, DMSO-d_6) of aquated complex **1c**, L-proline and L-cysteine amino acid molecules upon incubation for a period of 24 h at 313 K. The spectra show good similarity for complex **1c** signals between the aquated complex **1c** and that of **1c**-proline or **1c**-cysteine suggesting absence of bonded interactions between complex **1c** and these amino acids.

Interaction with histidine: Inspired by the formation of a coordination adduct on reacting with imidazole to form k^{1}N-imidazolyl complex. Interaction of complex **1a** and **1c** with histidine occurred with varying degrees in a time-dependent manner upon incubation of the mixture at 313 K for an extended period of 240 h. For complex **1c**, small amount of covalently bonded 1c-histidine adduct (*ca*. 9 %) through *N*1 or *N*3 was only observed after 192 h (**Figure S26**); with less than 2 % of the adduct observed after 96 h. In contrast, complex **1a** was observed to significantly interact with L-histidine to form k^{1}N-1a-histidine adduct within the first 96 h (**Figure S27**), suggesting the possibility of complex **1a** to readily interact with biomolecules such as serum proteins to a good extent under physiological conditions.

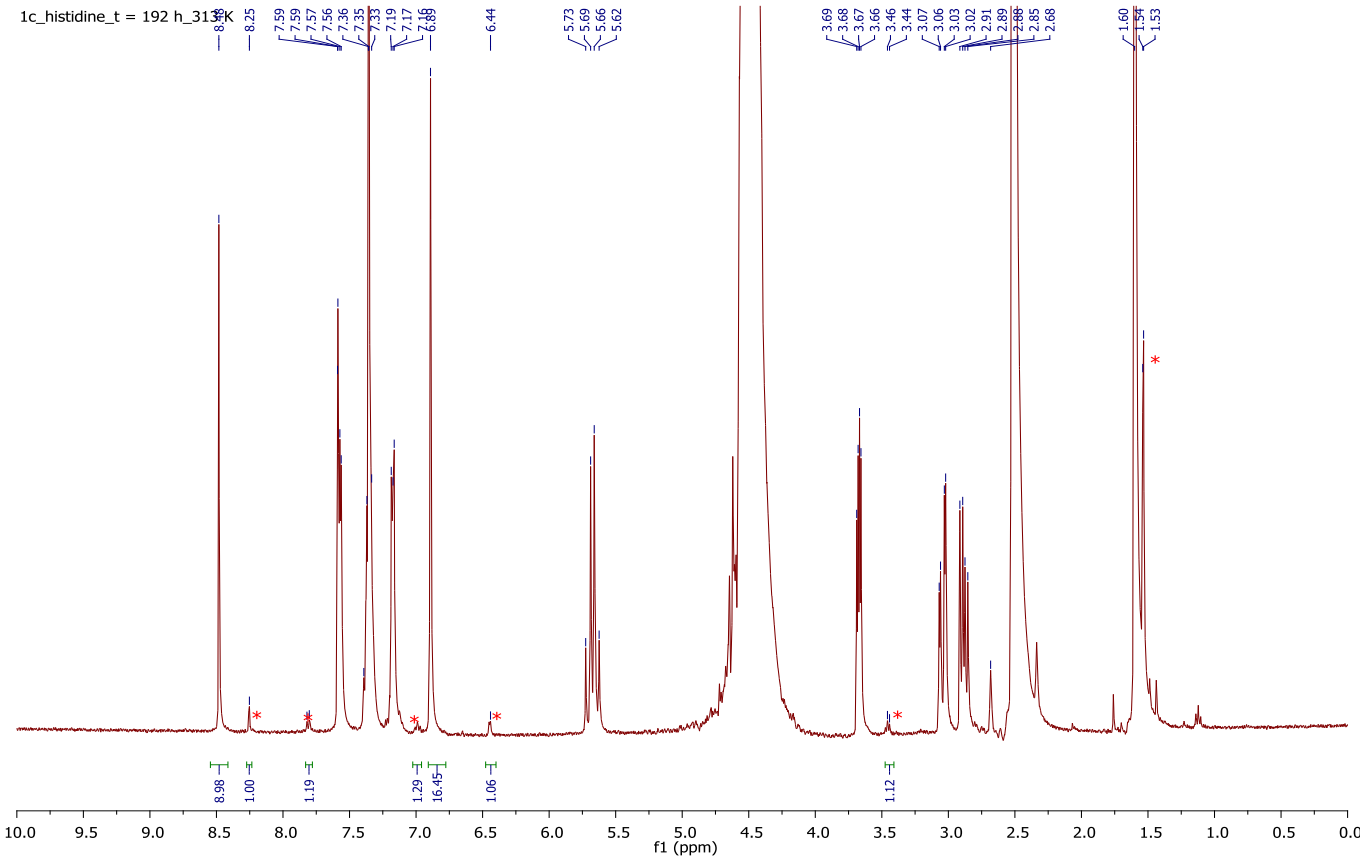

Figure S26: ^{1}H NMR spectrum (400 MHz, DMSO-d_6) of a mixture of complex **1c** and L-histidine amino acid recorded after 192 h showing traces (< 10 % w.r.t **1c**) of coordination complex k^1*N*-**1c**-histidine (*). There was less than 2 % of the adduct observed after 96 h of incubation of the mixture at 313 K.

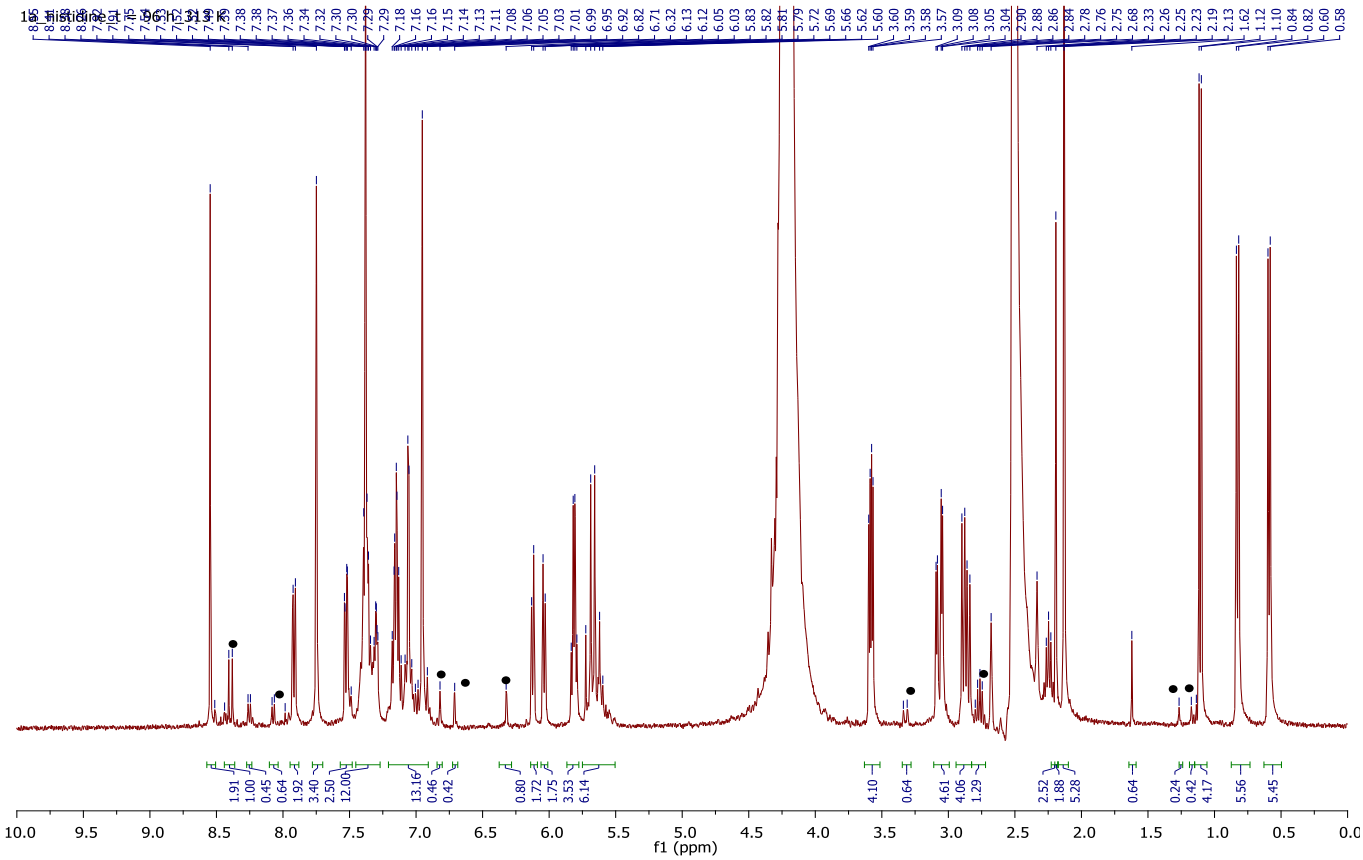

Figure S27: ^{1}H NMR spectrum (400 MHz, DMSO-d_6) of a mixture of complex **1a** and L-histidine amino acid recorded after 96 h upon incubation at 313 K, showing significant amount (> 30 %) of coordination adduct k^1N-1a-histidine evidenced by the emergence of a second set of peaks (●).

SUPPORTING INFORMATION

Scrambling Experiments: competitive experiments between amino acid and DNA model guanosine biomolecules: reveals selectivity to DNA model guanosine over amino acids within the experimental time of 24 h.

Scheme S2**:** Scrambling experiments of **1c** involving proline and 5'-GMP

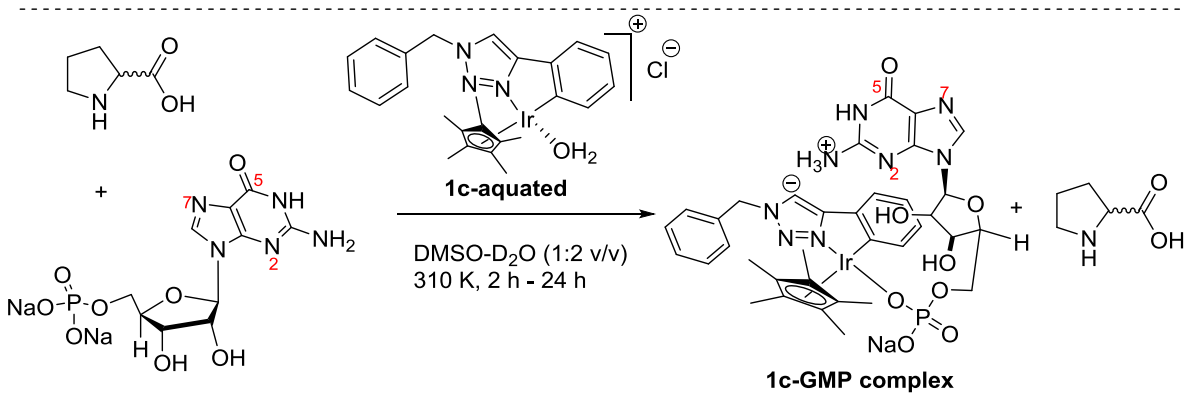

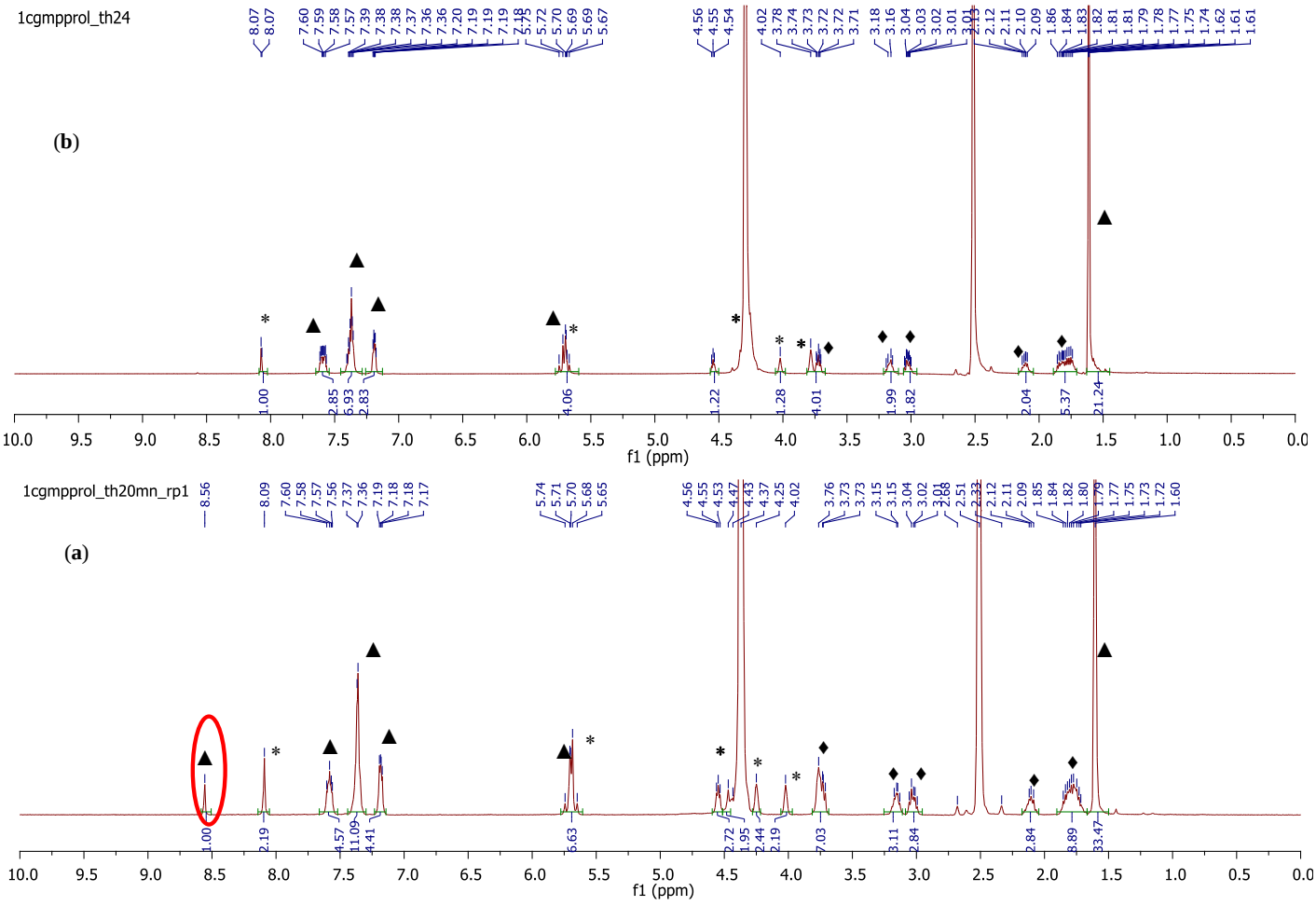

Figure S28: ^{1}H NMR spectrum (500 MHz, DMSO-d_6) of the reaction mixture of cyclometallated **1c (▲)**, L-proline (♦) and 5'-GMP (*) recorded after 24 hours of incubation at 310 K. Notably, the triazole proton H-5 (δ 8.56 ppm; circled in red) in (**a**) of the aquated complex **1c** disappeared after 24

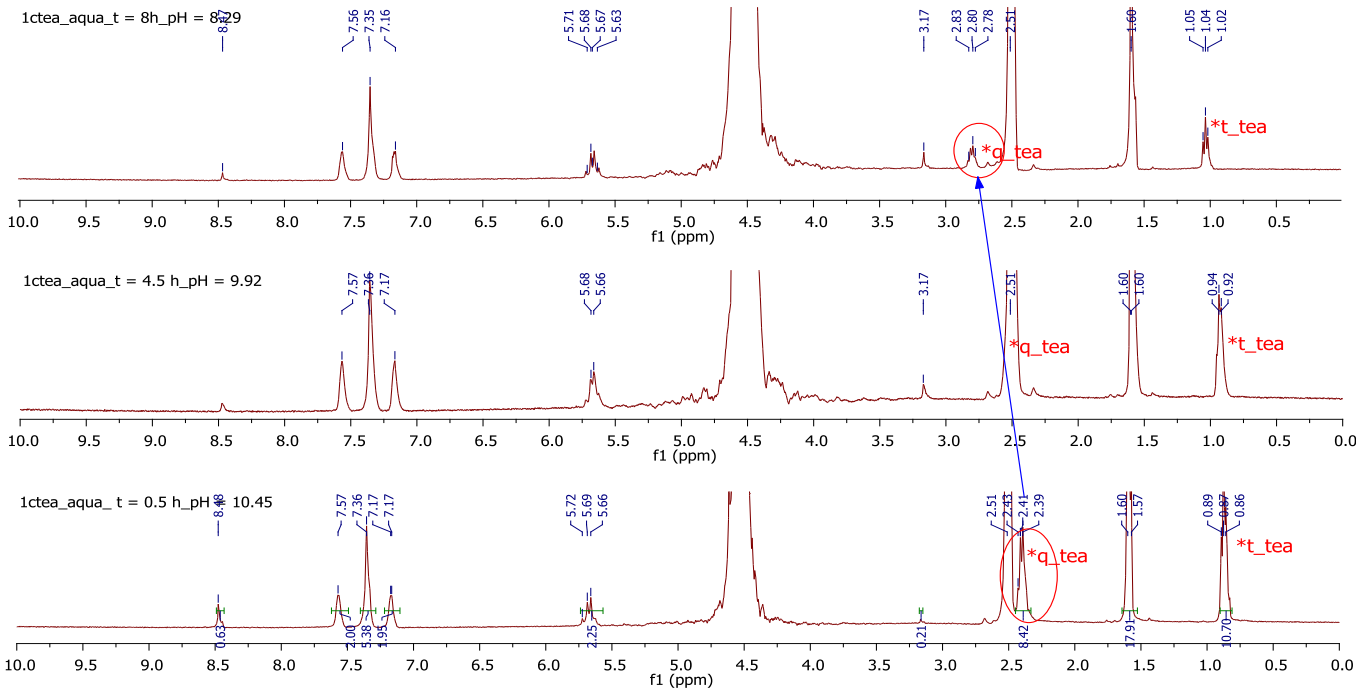

Figure S29: Time dependent ^{1}H NMR showing the interaction of triethyl amine base with aquated complex **1c**-H_2O leading to deprotonation of the triazole H-5 proton evidenced by the decreasing intensity of (or rather area under) the triazole proton H-5 signal and the downfield shift of methylene protons ($\Delta\delta$ = + 0.39 ppm; red circle: from δ_H 2.41 ppm → δ_H 2.80 ppm) of triethyl amine corresponding to protonated triethyl amine.

SUPPORTING INFORMATION

1D NOESY experiments: Transient NOEs for **1a_I** and **1a_II** on selective irradiation of δ_H 7.52 ppm (i.e. triazole proton H-5) are shown in Figure S7 using a mixing time, d8 = 0.3s. Build up experiments at different mixing times (d8 = 0.01s -1s) and 2D-NOESY were used to establish appropriate NOEs from artifacts. The % NOE was estimated by calculating percent integral ratio of the NOE peak to that of the saturation peak.

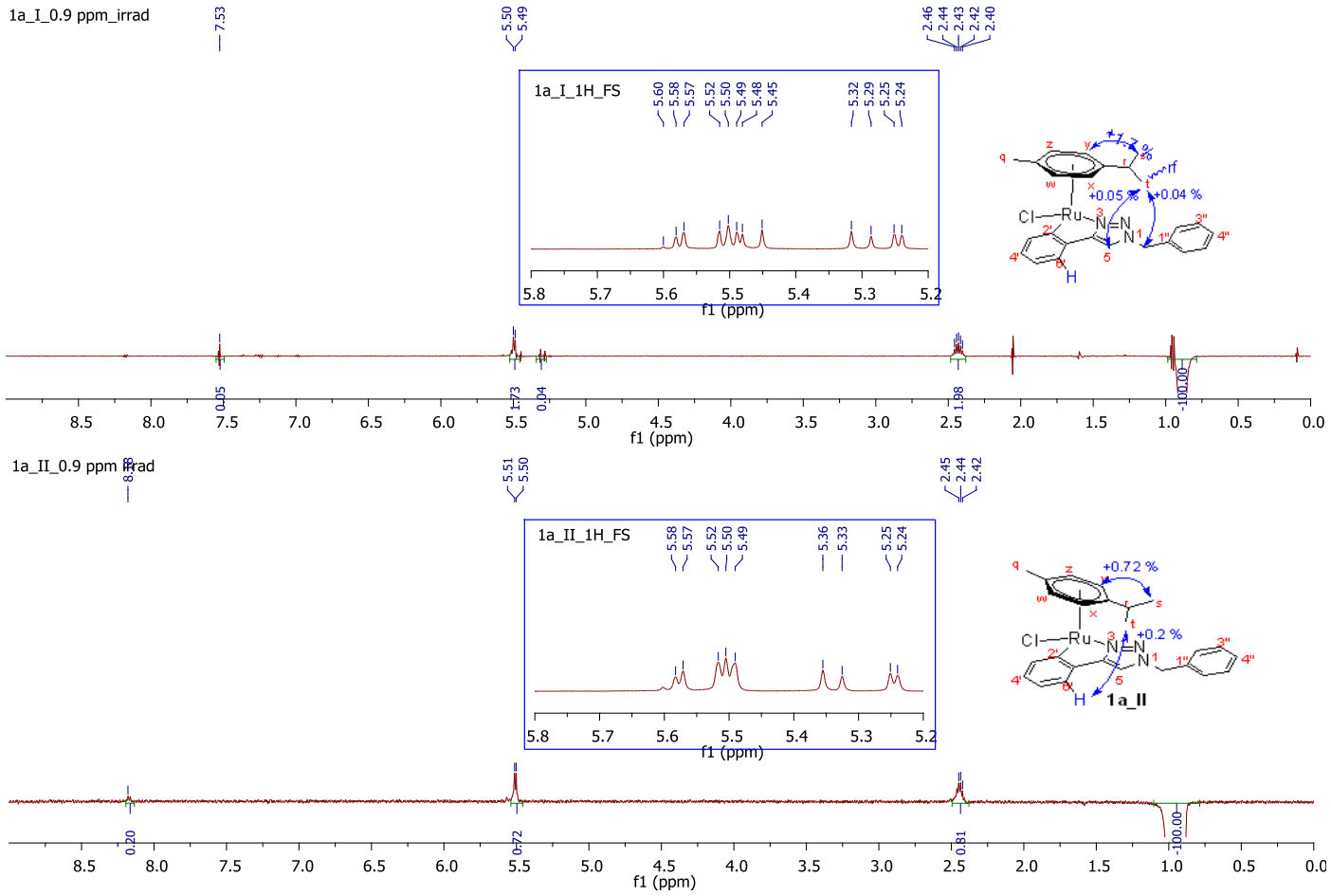

Figure S30: ^{1}H NMR spectra (500MHz, $CDCl_3$) of stereoisomers of **1a** showing distinct nuclear Overhauser effects on metallated phenyl protons upon irradiation of the methyl region of the isopropyl group (*p*-cymene); isomer **1a_I** (upper spectrum) with no NOE on H-6' and **1a_II** (lower spectrum) exhibit +0.2 % NOE on H-6'. Insert: A section (δ 5.2 – 5.8 ppm) of the full spectrum for each of the isomers.

BEHAVIOR OF THE COMPLEX OF 1c IN THE PRESENCE OF BSA: UV-VIS SPECTROPHOTOMETRY

UV-Vis Spectroscopic BSA-1c titration. Treatment of 1% DMSO-PBS solution of BSA with various concentrations (2.5 μM, 5 μM, 7.5 μM, 8 μM, 9 μM, 10 μM and 12.5 μM) of 1% DMSO-PBS solution of complex **1c** gave the absorption curves shown in Figure **1b**. The absorption intensity of BSA-**1c** complex increased with increasing concentration of complex **1c**. The absorption peaks at λ = 239.50 nm and λ = 278.50 nm are ascribed to the peptide and the aromatic ring of the aromatic amino acids, respectively.[1]

SUPPORTING INFORMATION

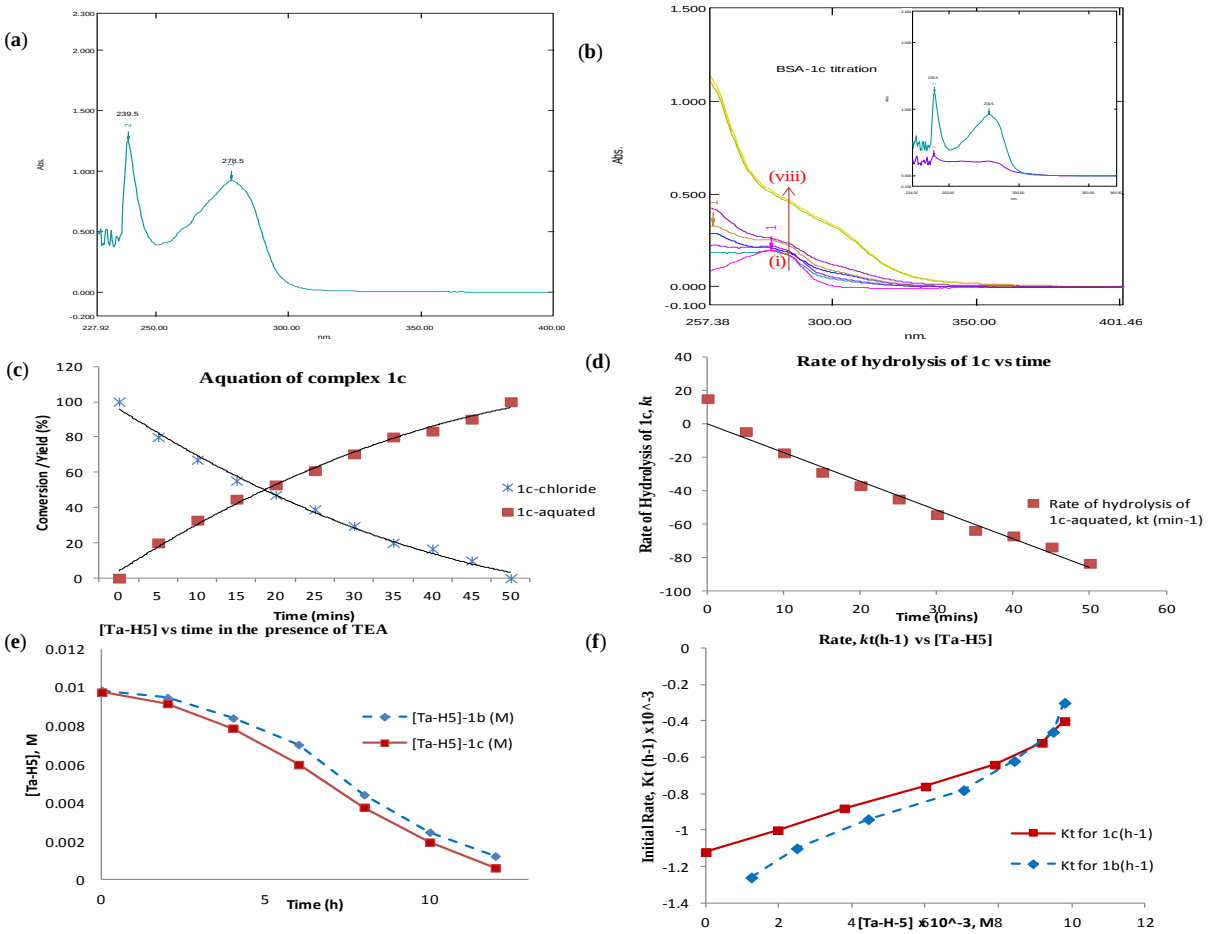

Figure S31: UV-Vis absorption curves of (a) 10 μM BSA only (b) BSA titration curves with 1c: (i) BSA only (2 μM) and BSA with (ii) 5 μL (iii) 10 μL (iv) 15 μL (v) 16 μL (vi) 18 μL, (vii) 20 μL and (viii) 25 μL of 2 mM stock 1 % DMSO-PBS (pH 7.4) solution of complex 1c. 1% DMSO-PBS solution was used as the reference solution. **Inset**: An overlay of BSA only (green; 10 μM BSA) and BSA (2uM) + **1c** (10 μM) spectra. (c) Relative conversion of complex **1c** (■) to the cationic aquated complex (*), **1c**(OH_2)Cl. (d) Rate of hydrolysis of the chloride complex **1c** to form the aquated complex; rate constant, k_{hyd} =1.8293 min^{-1} or 109.758 h^{-1} based on time-dependent consumption of complex **1c**. (e) Variations in concentration of triazole proton H-5, [Ta-H5], with time for complexes **1b** (blue) and **1c** (red) in carbenylation, monitored using ^{1}H NMR spectroscopy. (f) Rate of deprotonation, k_t, of triazole proton H-5 with time; rate constant, k_d = 8.0 x 10^{-4} s^{-1} or 2.88 h^{-1} for complex **1c**.

From UV-Vis spectrophotometric studies, compound **1c** shows possibly weak or no interaction with bovine serum albumin (BSA) as a model protein following the insignificant changes in the absorption wavelengths of the peptide (λ = 239.5 nm) and the aromatic moieties of the protein (λ = 278.5 nm) (Figure **1a** and **1b**).

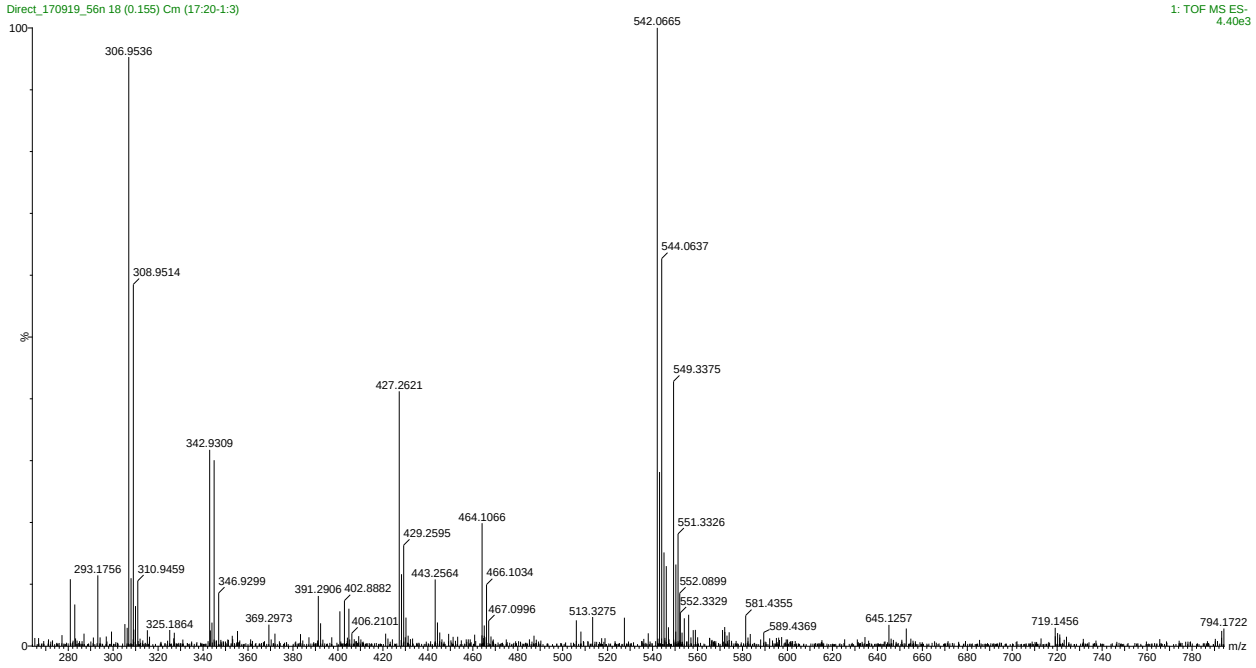

Figure S32: HRMS-ESI(-ve) spectrum for cyclometallated 1-benzyl-4-phenyl-1*H*-1,2,3-triazolyl (pentamethylcyclopentadienyl)rhoddium(III) chloride complex **1b** showing a peak at *m/z* 542.0665 corresponding to $C_{25}H_{27}RhClN_3$ $[M+Cl]^-$, (calcd *m/z* 542.0637).

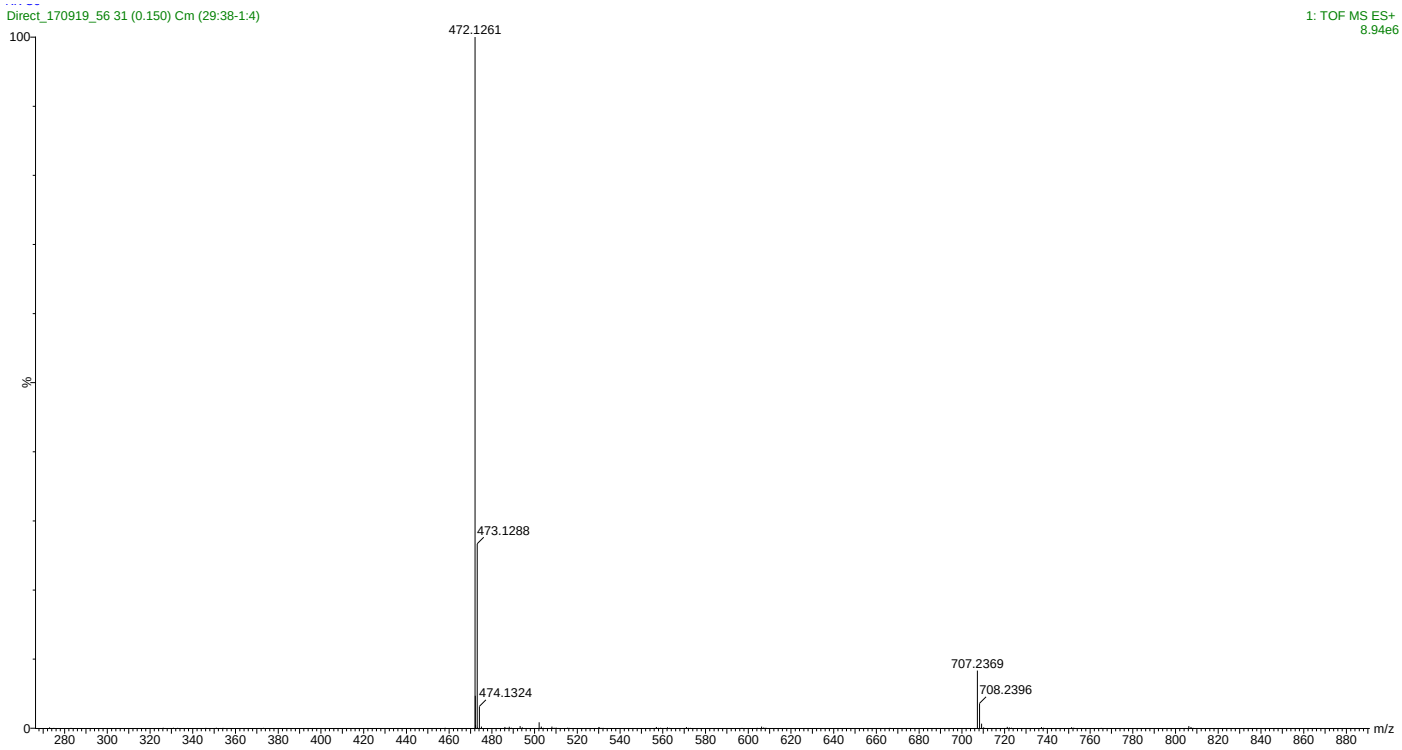

Figure S33: HRMS-ESI(+ve) spectrum for cyclometallated 1-benzyl-4-phenyl-1*H*-1,2,3-triazolyl (pentamethylcyclopentadienyl)rhoddium(III) chloride complex **1b** showing a base peak at *m/z* 472.1261 corresponding to $C_{25}H_{27}RhN_3$ $[M-Cl]^+$, (calcd *m/z* 472.1260).

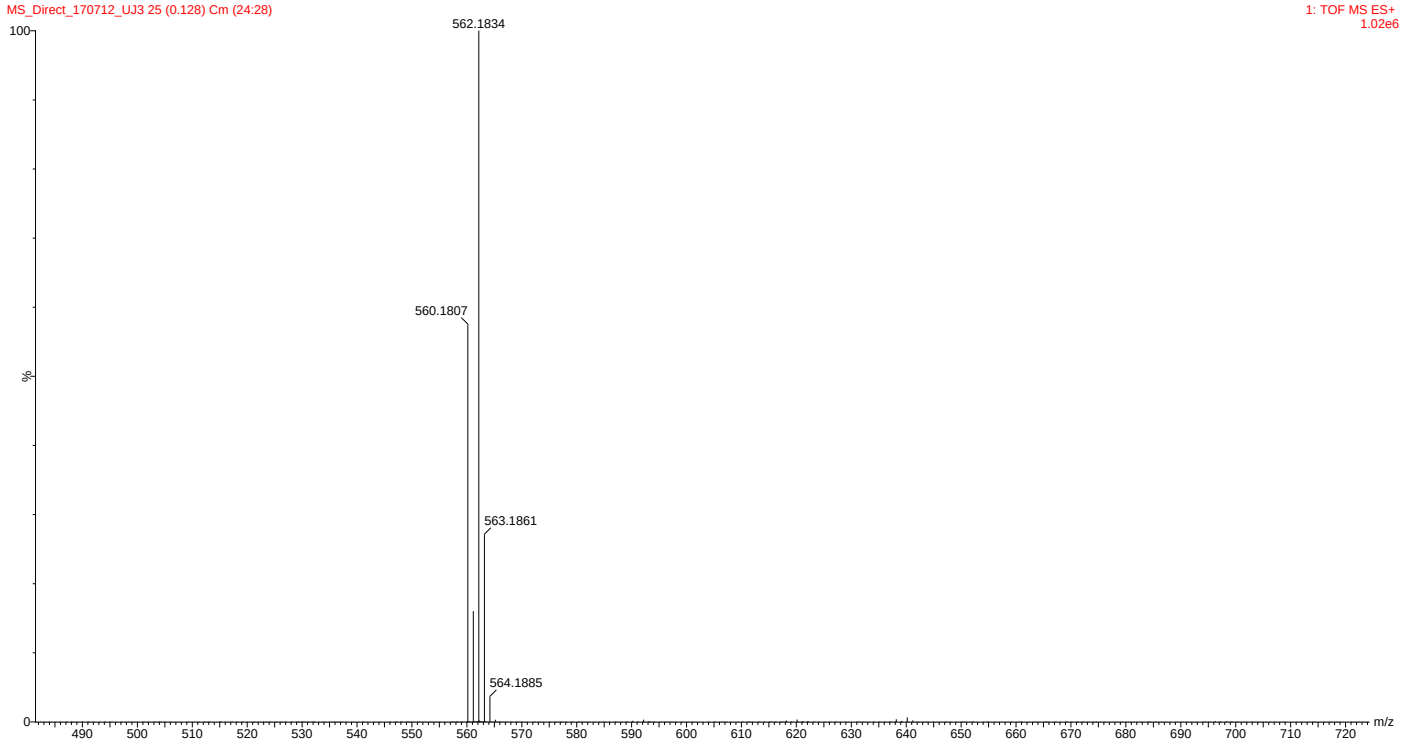

Figure S34: HRMS-ESI(+ve) spectrum for cyclometallated 1-benzyl-4-phenyl-1*H*-1,2,3-triazolyl (pentamethylcyclopentadienyl)iridium(III) chloride complex **1c** showing a base peak at *m/z* 562.1834 corresponding to $C_{25}H_{27}IrN_3$ [M-Cl]$^+$, (calcd *m/z* 562.1834).

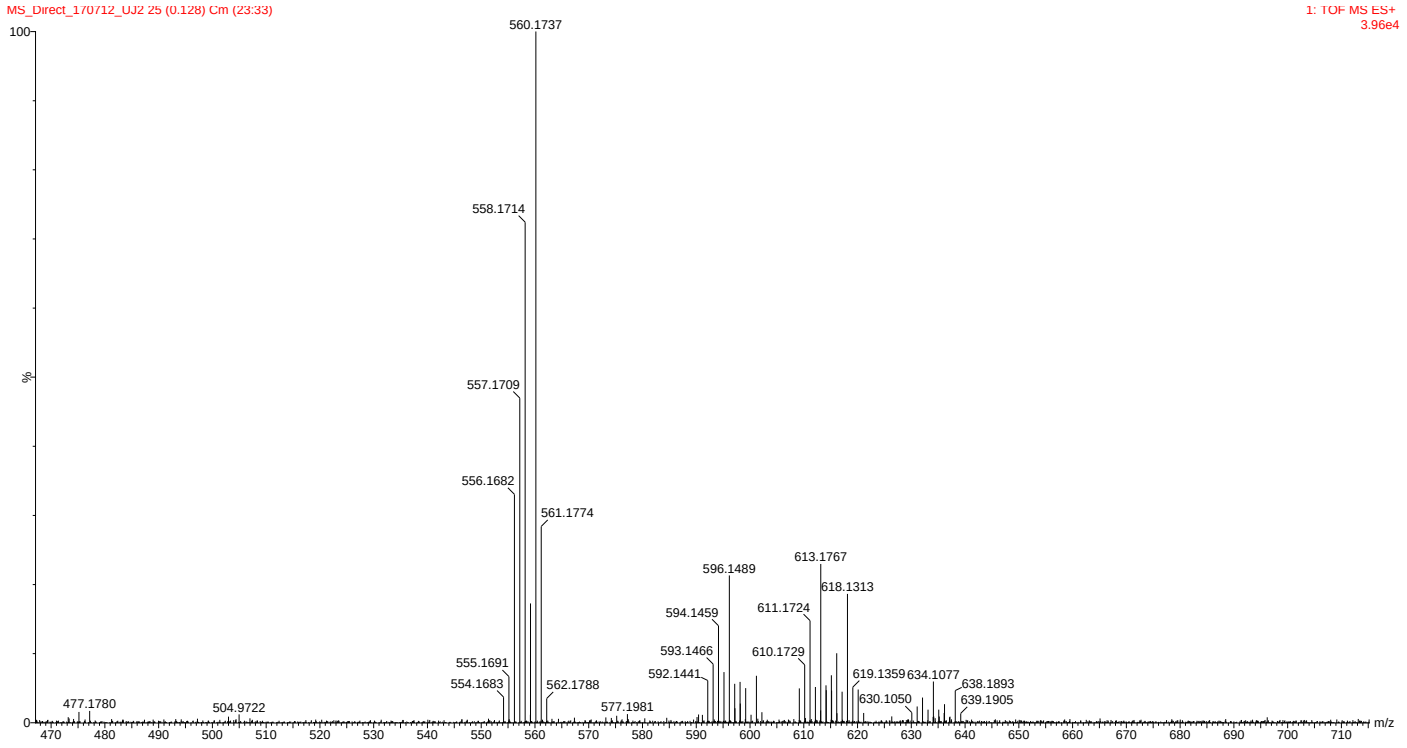

Figure S35: HRMS-ESI(+ve) spectrum for cyclometallated 1-benzyl-4-phenyl-1*H*-1,2,3-triazolyl(*p*-cymene)osmium(II) chloride complex **1d** showing a base peak at *m/z* 560.1737 corresponding to $C_{25}H_{28}N_3Os$ [M-Cl]$^+$, (calcd *m/z* 560.1868).

REFERENCES

1. Zhang, Y.; Zhong, Q., Binding between bixin and whey protein at pH 7.4 studied by spectroscopy and isothermal titration calorimetry. *J. Agric. Food. Chem.* **2012,** *60* (7), 1880-1886.